Photoinduced Electron Transfer in Eosin-Modified Co(II)-Protoporphyrin IX Reconstituted Myoglobin and α- or β-Hemoglobin Subunits: Photocatalytic Transformations by the Reconstituted Photoenzymes[1]

Eran Zahavy and Itamar Willner*,†

Contribution from the Institute of Chemistry and Farkas Center for Light Induced Processes, The Hebrew University of Jerusalem, Jerusalem 91904, Israel

Received March 18, 1996[⊗]

Abstract: A series of hemo-protein-derived photocatalysts, prepared by reconstitution of the respective apo-proteins with Co(II)-protoporphyrin IX and chemical modification of the protein with the eosin chromophore, is presented. Apo-myoglobin, Apo-Mb, was reconstituted with Co(II)-protoporphyrin IX and further modified with eosin-isothiocyanate (**3**) to yield the photocatalyst Eo^{2-}-Mb-Co(II). The protein is loaded by two eosin chromophore units. Photoexcitation of Eo^{2-}-Mb-Co(II) yields the electron transfer species $Eo^{\bullet-}$-Mb-Co(I) formed by direct oxidative quenching of $^{T}Eo^{2-}$-Mb-Co(II), $k_q = 5.2 \times 10^4$ s^{-1}, and via an indirect path where self-quenching of the eosin-chromophore units yields the intermediate redox products ($Eo^{\bullet 3-}$ + $Eo^{\bullet-}$)-Mb-Co(II) that, in the presence of Na_2-EDTA, generate the $Eo^{\bullet-}$-Mb-Co(I) in a secondary dark electron transfer, $k_r = 330$ s^{-1}. The reconstituted protein Eo^{2-}-Mb-Co(II) reveals photocatalytic features and its steady-state illumination in the presence of Na_2EDTA yields hydrogen evolution, $\phi = 2 \times 10^{-4}$, or photohydrogenation of acetylene to ethylene, $\phi = 1 \times 10^{-2}$. The reconstituted photocatalyst Eo^{2-}-Mb-Co(II) reveals enzyme-like behavior. Photohydrogenation of acetylenedicarboxylic acid (**6**) by Eo^{2-}-Mb-Co(II) in the presence of Na_2EDTA reveals stereospecificity and formation of maleic acid as the hydrogenation product and kinetics that follow the Michaelis−Menten model, $K_m = 4$ mM, $V_{max} = 0.6$ μM·min^{-1}. Similarly, the α- and β-subunits of hemoglobin, Hb, were reconstituted with Co(II)-protoporphyrin IX to yield α-Hb-Co(II) and β-Hb-Co(II). The β-Hb-Co(II) was specifically modified at cysteine 93 residue by eosin maleimide (**4**) to form Eo^{2-}-β-Hb-Co(II). The α-Hb-Co(II) was modified at a single, unknown, lysine residue by eosin maleimide (**4**) to generate Eo^{2-}-α-Hb-Co(II). Only oxidative quenching proceeds in Eo^{2-}-β-Hb-Co(II) and Eo^{2-}-α-Hb-Co(II) to yield the redox photoproducts, $Eo^{\bullet-}$-β-Hb-Co(I) and $Eo^{\bullet-}$-α-Hb-Co(I), $k_q^{\beta} = 1.8 \times 10^3$ s^{-1} and $k_q^{\alpha} = 6.5 \times 10^3$ s^{-1}, respectively. The back electron-transfer rates of the redox species are $k_b^{\beta} = 0.37 \times 10^3$ s^{-1} and $k_b^{\alpha} = 3.4 \times 10^3$ s^{-1}, respectively. The site-specific modification at cysteine 93 residue of β-Hb by the chromophore and the known X-ray structure of β-Hb which defines the electron transfer distance in Eo^{2-}-β-Hb, $d = 12.87$ Å, enabled the analysis of the experimental electron-transfer rate constants according to Marcus theory: $\lambda = 1.1$ eV; $\beta = 1.35$ Å^{-1}. The reorganization energy, λ, associated with the electron transfer in Eo^{2-}-α-Hb-Co(II) is similar, $\lambda = 1.15$ eV. Application of the β-value extracted for the Eo^{2-}-β-Hb-Co(II) system to the Eo^{2-}-α-Hb-Co(II) assembly enabled estimation of the electron-transfer distance in the latter system, $d = 11.2$ Å, and elucidation of the lysine-90 residue as the modification site by the eosin chromophore. The two reconstituted proteins, Eo^{2-}-α-Hb-Co(II) and Eo^{2-}-β-Hb-Co(II), reveal photocatalytic properties. Their steady-state irradiation in the presence of the Na_2EDTA resulted in photohydrogenation of acetylene to ethylene, $\phi^{\alpha} = 0.02$; $\phi^{\beta} = 0.004$. The photogenerated redox species of the reconstituted proteins $Eo^{\bullet-}$-Mb-Co(I) and $Eo^{\bullet-}$-α/β-Hb-Co(I) reveal pronounced stabilities against back electron transfer. This was attributed to spatial separation of the redox species by the rigid protein assemblies. The stability of the redox photoproducts $Eo^{\bullet-}$-Mb-Co(I) enabled tailoring a cyclic photosynthetic assembly where the semisynthetic photoenzyme Eo^{2-}-Mb-Co(II) as a reductive biocatalyst is coupled to lactate dehydrogenase, LDH, an oxidative biocatalyst, using *N*-methylferrocene caproic acid (**5**) as diffusional electron mediator. Steady-state irradiation of an assembly composed of Eo^{2-}-Mb-Co(II), LDH, and **5** in the presence of acetylene and lactic acid yields the cyclic photoinduced hydrogenation of acetylene by lactic acid to yield ethylene and pyruvic acid, $\phi = 2 \times 10^{-3}$. The system mimics artificially the functions of the photosynthetic bacteria chloroflexus.

Introduction

Long-range electron transfer reactions represent an active theoretical[2] and experimental research effort.[3,4] Marcus theory predicts[2] that electron transfer rate between a donor−acceptor pair embedded in a protein is given by eq 1, where $\Delta G°$ and λ are the free energy change and reorganization energy associated with the electron transfer, d_o and d are the van der Waals donor−acceptor distance and the actual distance separating the donor−acceptor, respectively, and β is the distance-dependent electron coupling constant between the donor and the acceptor. Ingenious experiments attempting to characterize electron transfer

† Fax # 972-2-6527715. Tel # 972-2-6585272.

⊗ Abstract published in *Advance ACS Abstracts,* November 15, 1996.

(1) For preliminary reports see: (a) Willner, I.; Zahavy, E.; Heleg-Shabtai, V. *J. Am. Chem. Soc.* **1995**, *117*, 542−543. (b) Zahavy, E.; Willner, I. *J. Am. Chem. Soc.* **1995**, *117*, 10581−10582.

(2) (a) Marcus, R. *J. Chem. Phys.* **1956**, *24*, 966−971. (b) Marcus R.; Sutin, N. *Biochim. Biophys. Acta* **1985**, *811*, 265−312. (c) Jortner, J.; Bixon, M. In *Protein Structure: Molecular and Electronic Reactivity*; Austin, R., Buhks, E., Chance, B., De Vault, D., Dutton, P. L., Frauenfelder, H., Gol'danskii, V. I., Eds.; Springer-Verlag: New York 1987; pp 277−308. (d) Bixon, M.; Jortner, J.; Michel-Beyerle, M. E.; Ogrodnik, A. *Biochim. Biophys. Acta* **1989**, *977*, 273.

S0002-7863(96)00871-2 CCC: $12.00

rates in proteins were carried out. These included the site-

$$k_{ET} \propto \exp\{-\beta(d - d_o\}\cdot\exp\left\{-\frac{(\Delta G^\circ + \lambda)^2}{4\lambda k_B T}\right\} \qquad (1)$$

specific modification of proteins, i.e., cytochrome *c*,[5] myoglobin or hemoglobin,[6] with photoactive or electroactive groups and examination of the electron-transfer quenching and back electron transfer in the resulting proteins. Similarly, the light-induced electron transfer quenching and back electron transfer were studied in reconstituted redox proteins, i.e., cytochrome *c*, that include photoactive porphyrin analogs and electron acceptor units.[7] Although the electron transfer rates in various series of proteins followed Marcus theory, other systems revealed discrepancy. Recent advances in the topic suggested that in addition to the spatial (distance) separation of the donor−acceptor pair, other parameters such as the ordering of the amino acids in the protein, intraprotein hydrogen bonds separating the donor−acceptor pair,[8] and conformational dynamics of the donor−acceptor units,[9] are characteristic factors that control the electron transfer paths in proteins.

Electron transfer between the redox-center of proteins and their macroscopic surrounding is another important aspect. Usually, the redox-active centers of proteins are shielded towards electrical communication with the external macroscopic phase. This originates from the fact that the protein matrix spatially separates (distance separation) its redox center from the external surrounding.[10] Nature has developed means to control electrical communication of the redox-site of enzymes and their environment. This is achieved by the participation of protein-associated cofactors, i.e., FAD or PQQ or diffusional cofactors, i.e., NAD(P)H/NAD(P)$^+$, acting as electron (or hole) carriers through the protein. Substantial efforts are directed to develop electrochemical, photochemical and chemical means for the regeneration of NAD(P)$^+$/NAD(P)H cofactors and their use in biocatalyzed transformations.[11] Also, electrical wiring of redox enzymes with their exterior environment, i.e., electrode surfaces, generated experimental efforts since the resulting enzyme electrode assemblies can act as amperometric biosensor devices.[11,12] Various electron mediators of appropriate size, electrical charge and hydrophobicity act as diffusion electron carriers for redox proteins. These components penetrate the protein and shuttle the electrons to or from the active site. *N,N′*-Dialkyl-4,4′-bipyridinium salts,[13] ferrocene,[14] quinones[15] and tungsten or molybdenum octacyanides[16] were applied as synthetic electron mediators that electrically communicate redox proteins by a diffusional path in electrochemical, photochemical or chemical assemblies. An alternative method to establish electrical contact of redox enzymes and their surrounding includes the chemical modification of the protein with electron carrier units. In these systems, electron transfer proceeds by "electron hopping" through a series of relay units, located at relatively short distances, to or from the enzyme redox center. This approach was successfully applied to electrically communicate redox enzymes and electrode surfaces,[17] as well as to photochemically activate redox proteins, i.e., photobiocatalyzed reduction of oxidized glutathione.[18] Recently, a novel method to transform redox enzymes into "electroenzyme" biocatalysts was reported by the reconstitution of apo-flavo-enzymes with a relay-modified FAD cofactor[19] as well as by the reconstitution of the apo-enzyme onto relay-modified-FAD monolayers associated with electrode surfaces.[20]

Recently, it was demonstrated that chemical modification of redox-enzymes, i.e., glutathione reductase with chromophore units, enabled electron transfer communication between the redox-center and the excited chromophore.[21] This turns the enzyme into a light-activated biocatalyst, "photoenzyme". Here we report on a novel method to tailor photoenzymes by the reconstitution[22] of hemoproteins with a catalytic Co(II)-protoporphyrin IX redox site, and further modification of the protein with chromophore units. This concept is schematically outlined in Figure 1 where photoexcitation of the chromophore, S, induces electron transfer to the Co(II)-protoporphyrin IX site that effects the photobiocatalyzed reduction of a substrate (acetylene). This method is described with the reconstitution of apo-hemoglobin and apo-α- and β-subunits of hemoglobin with Co(II)-protoporphyrin IX. The reconstituted proteins are further modified with the eosin chromophore to yield the photoactive biocatalysts. A detailed analysis of the electron

(3) (a) McLendon, G. *Acc. Chem. Res.* **1988**, *21*, 160−167. (b) McLendon, G.; Guarr, T.; McGuire, M.; Simolo, K.; Strauch, S.; Taylor, K. *Coord. Chem. Rev.* **1985**, *64*, 113−124. (c) *Electron Transfer in Biology and the Solid State*; Johnson, M. K., King, R. B., Kurtz, D. M., Jr., Kutal, C., Norton, M. L., Scott, R. A., Eds.; American Chemical Society: 1990.

(4) (a) Winkler, J. R.; Gray, H. B. *Chem. Rev.* **1992**, 369−379. (b) Gray, H. B.; Malmström, Bo-G. *Biochemistry* **1989**, *19*, 7499−7505. (c) Isied, S. S.; Ogawa, M. Y.; Wishart, J. W. *Chem. Rev.* **1992**, *92*, 381.

(5) (a) Yocom, K. M.; Shelton, I. B.; Shelton, J. R.; Schroeder, W. A.; Worosila, G.; Isied, S. S.; Bordignon, E.; Gray, H. B. *Proc. Natl. Acad. Sci. U.S.A.* **1982**, *79*, 7052−7055. (b) Durham, B.; Pan, L.-P.; Long, J. E.; Millet, F. *Biochemistry* **1989**, *28*, 8659−8665. (c) Chang, I-Jy.; Gray, H. B.; Winkler, J. R. *J. Am. Chem. Soc.* **1991**, *113*, 7056−7057.

(6) (a) Liang, N.; Grant Mauk, A.; Pielak, G. R.; Johnson, J. A.; Smith, M.; Hoffman, B. M. *Science* **1988**, *240*, 311−313. (b) Casimiro, D. R.; Wong, L. L.; Colon, J. L.; Zewert, T. E.; Richards, J. H.; Chang, I.-J.; Winkler, J. R.; Gray, H. B. *J. Am. Chem. Soc.* **1993**, *115*, 1485−1489. (c) Peterson-Kennedy, S. E.; McGourty, J. L.; Ho, P. S.; Sutoris, C. J.; Liang, N.; Zemel, H.; Blough, N. V.; Margoliash, E.; Hoffman, B. M. *Coord. Chem. Rev.* **1985**, *64*, 125−133.

(7) (a) Therien, M. J.; Selman, M.; Gray, H. B.; Chang, I-Jy.; Winkler, J. R. *J. Am. Chem. Soc.* **1990**, *112*, 2420−2422. (b) Meade, T. J.; Gray, H. B.; Winkler, J. R. *J. Am. Chem. Soc.* **1989**, *111*, 4353−4356. (c) McLendon, G.; Miller, J. R. *J. Am. Chem. Soc.* **1985**, *107*, 7811−7816.

(8) (a) Beratan, D. N.; Betts, J. N.; Onuchic, J. N. *Science* **1991**, *252*, 1285−1288. (b) Skourtis, S. S.; Regna, J. J.; Onuchic, J. N. *J. Phys. Chem.* **1994**, *98*, 3379−3388.

(9) Conrad, D. W.; Zhang, H.; Stewart, D. E.; Scott, R. A. *J. Am. Chem. Soc.* **1992**, *114*, 9909−9915.

(10) Heller, A. *Acc. Chem. Res.* **1990**, *23*, 128.

(11) (a) Willner, I.; Willner, B. In *Topics in Current Chemistry: Photoinduced Electron Transfer III*; Mattay, J., Ed.; Springer-Verlag: Berlin, 1991; Vol. 159, pp 153−218. (b) Willner, I.; Mandler, D. *Enzyme and Microbial. Tech.* **1989**, *11*, 467−483.

(12) Heller, A. *J. Phys. Chem.* **1992**, *96*, 3579.

(13) (a) Mandler, D.; Willner, I. *J. Chem. Soc., Perkin Trans. 2* **1988**, 997. (b) Adams, M. W. W.; Rao, K. K.; Hall, D. O. *Photobiochem. Photobiophys.* **1979**, *1*, 33. (c) Okura, I.; Takeuchi, M.; Kim-thuan, N. *Chem. Lett.* **1980**, 765. (d) Willner, I.; Lapidot, N.; Riklin, A. *J. Am. Chem. Soc.* **1989**, *111*, 1883.

(14) Yeh, P.; Kuwana, T. J. *Electrochem. Soc.* **1976**, *123*, 1334.

(15) Ikeda, T.; Hiasa, H.; Senda, M. In *Redox Chemistry and Interfacial Behavior of Biological Molecules*; Dryhurst, G., Niki, K., Eds.; Plenum Publ. Corp.: New York, 1988; pp 193−201.

(16) Taniguchi, I.; Miyamoto, S.; Tomimura, S.; Hawkridge, F. M. J. *Electroanal. Chem. Interfacial Electrochem.* **1988**, *240*, 333.

(17) (a) Degani, Y.; Heller, A. *J. Am. Chem. Soc.* **1988**, *110*, 2615−2620. (b) Degani, Y.; Heller, A. *J. Phys. Chem.* **1987**, *91*, 1285−1289. (c) Riklin, A.; Willner, I. *Anal. Chem.* **1995**, *67*, 4118−4126. (d) Shoham, B.; Migron, Y.; Riklin, A.; Willner, I.; Tartakovsky, B. *Biosensors Bioelectronics* **1995**, *10*, 341−352. (e) Willner, I.; Willner, B. *Adv. Mater.* **1995**, *7*, 587−589.

(18) Willner, I.; Lapidot, N.; Riklin, A. Kasher, R.; Zahavy, E.; Katz, E. *J. Am. Chem. Soc.* **1994**, *116*, 1428−1441.

(19) Riklin, A.; Katz, E.; Willner, I.; Stocker, A.; Bückmann, A. F. *Nature* **1995**, *376*, 672−675.

(20) Willner, I.; Heleg-Shabtai, V.; Blonder, R.; Katz, E.; Tao, G.; Bückmann, A. F.; Heller, A. *J. Am. Chem. Soc.* **1996**, *118*, 10321−10322.

(21) Willner, I.; Zahavy, E. *Angew Chem., Int. Ed. Engl.* **1994**, *33*, 581−583.

(22) For other photochemical studies with reconstituted myoglobin, see: (a) Hamachi, I.; Tanaka, S.; Shinkai, S. *J. Am. Chem. Soc.* **1993**, *115*, 10458−10459. (b) Hayashi, T.; Takimura, T.; Ogoshi, H. *J. Am. Chem. Soc.* **1995**, *117*, 11606−11607. (c) Hayashi, T.; Takimura, T.; Ohara, T.; Hitomi, Y.; Ogoshi, H. *J. Chem. Soc., Chem. Commun.* **1995**, 2503−2504.

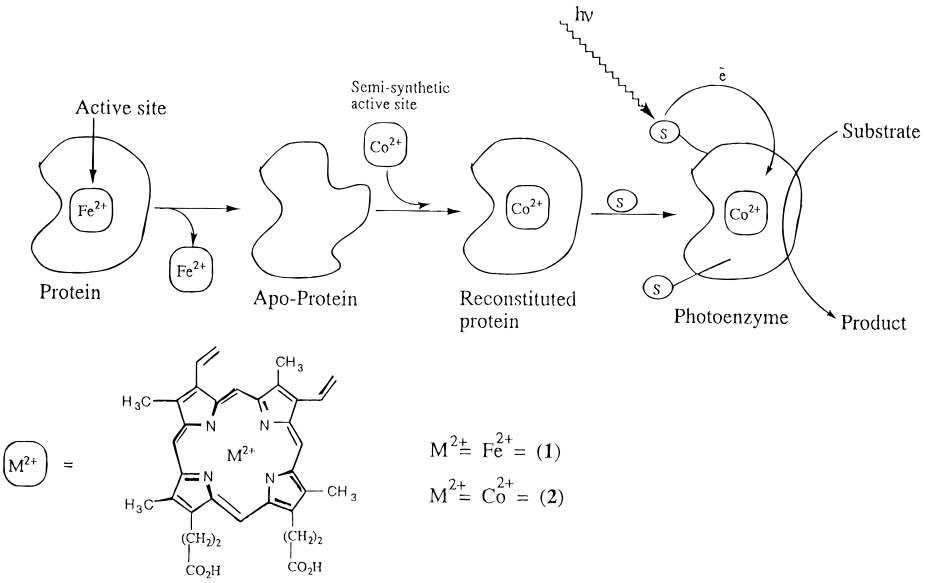

Figure 1. Design of a photoenzyme by reconstitution of a heme-protein by Co(II)-protoporphyrin IX and chemical modification of the protein backbone by a chromophore.

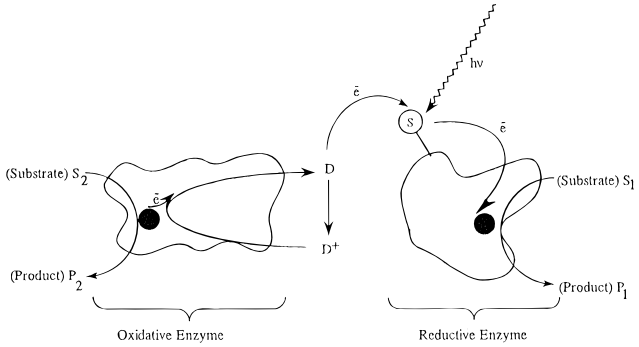

Figure 2. Cyclic photosynthetic assembly composed of a reductive photoenzyme and an oxidative biocatalyst.

transfer reaction in the semisynthetic enzymes is described, and the photobiocatalytic properties of the reconstituted proteins and steady-state irradiation are addressed. Furthermore, the semisynthetic photoenzyme is coupled to an external diffusional electron carrier that allows the cyclic photosynthesis. This concept of cyclic photosynthesis using a semisynthetic photoenzyme is schematically described in Figure 2. The system is composed of the photoenzyme acting as the reductive site and an oxidative enzyme acting as the oxidation site. Light-induced activation of the photoenzyme induces electron transfer and charge separation. The oxidized chromophore is reduced by a diffusional reversible electron carrier, D, and the oxidized electron mediator is specifically recognized by the oxidative enzyme that stimulates a biocatalyzed oxidation process. Thus, the diffusional electron mediator couples the reductive and oxidative biocatalysts. This approach is described by coupling the eosin-modified Co(II)-protoporphyrin IX-reconstituted myoglobin with lactate dehydrogenase, LDH, using a ferrocene derivative as diffusional electron mediator. Cyclic photoinduced oxidation of lactic acid by acetylene to form pyruvic acid and ethylene is described.

Experimental Section

Absorption spectra were recorded on a Uvikon-860 (Kontron) spectrophotometer. Electrochemical measurements were performed on a EG&G Electroanalyzer (Model 263) linked to a PC-486 computer and using electrochemical software (EG&G Model 270). Gas chromatography analyses were performed with a HP-5890 gas chromatograph equipped with a FID detector using a Poropak-N column for acetylene and ethylene detection and a Molecular Sieve 5 Å column and TCD detector for H_2 detection. HPLC analyses were performed with a Merck-Hitachi instrument equipped with a Shodex KC-811 anion exchange column, an optical detector (190−370 nm) and a conductivity detector (Knauer). Steady-state illuminations were performed with a 150W Xe-lamp (Oriel). The light was filtered through a $CuSO_4$ solution and appropriate optical filters (Schott) to select the desired incident wavelength region. Time-resolved flash photolysis experiments were performed with a Nd:YAG laser (Spectra-Physics Quanta-Ray, Model GCR 150, laser pulse width <5 ns). The detection system included a spectrophotometer (LKS-347, Applied Photophysics) linked to a digitizer (Tektronix-2430A) and a PC-386 computer for data acquisition and analysis. The laser and detection system is triggered by an external delay generator, Stanford DG-535.

Eosin-5-maleimide and fluorescein-5-isothiocyanate were purchased from Molecular Probes. All other chemicals were purchased from Aldrich or Sigma. Eosin-5-isothiocyanate was prepared by the addition of Br_2 (0.5 mL) to a solution of fluorescein-5-isothiocyanate.[23] The resulting red precipitate was washed with ethanol. Co(II)-protoporphyrin IX (**3**) was prepared[24a] by dropwise addition of a protoporphyrin IX solution (100 mg in 40 mL of acetic acid and 15 mL pyridine) to a Co(II) acetate solution (100 mg in 100 mL acetic acid), heated to 80−85 °C under argon. The metalation of the porphyrin was complete after 15 min. The resulting solution was cooled to room temperature and evaporated. The resulting residue was dissolved in a minimum volume of ethylacetate:acetic acid 6:1, and insoluble residues were excluded by precipitation with a centrifuge. To the resulting clear solution was added *n*-hexane (1.5 the volume of the original solution), and Co(II)-protoporphyrin IX precipitated upon cooling. The precipitate was separated by a centrifuge and dried under vacuum.

Preparation of apo-Myoglobin, Apo-Mb. The apo-Mb was prepared with slight modifications of the literature method.[25] Horse heart myoglobin (100 mg) was dissolved in 100 mL of 0.1 M HCl solution, 4 °C, and treated in a separating funnel with 2-butanone (100 mL) to extract the protoheme (**1**). The aqueous uncolored phase was washed further by two portions of 2-butanone. The resulting aqueous phase was dialyzed against a 0.01 M phosphate buffer solution, pH = 7.5 (three times against 2 L of phosphate buffer, each dialysis was

(23) Cherry, R. J.; Cogoli, A.; Oppliger, M.; Schneider, G.; Semenza, G. *Biochemistry* **1976**, *15*, 3653−3656.

(24) (a) Inubushi, T.; Yonetani, T. In *Methods in Enzymology*; Antonini, E., Rossi-Bernardi, L., Chiancone, E., Eds.; Academic Press: London, 1981; Vol. 76, pp 88−94. (b) Ascoli, F.; Rosaria, M.; Fanelli, R.; Antonini, E. In *Methods in Enzymology*; Antonini, E., Rossi-Bernardi, L., Chiancone, E., Eds.; Academic Press: London, 1981; Vol. 76, pp 72−87.

(25) Teale, F. W. J. *Biochim. Biophys. Acta* **1959**, *35*, 543.

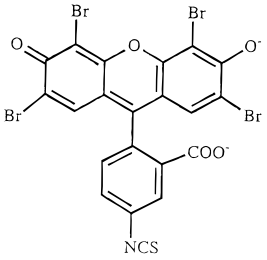

(3)

conducted for 3 h). The resulting Apo-Mb solution was lyophilized and the solid was stored at −18 °C.

Preparation of Co(II)-Protoporphyrin IX Reconstituted Mb, Mb-Co(II). The reconstitution of the apo-myoglobin with the Co(II)-protoporphyrin IX, (**2**), was performed under anaerobic conditions at 4 °C, following the literature method.[24b] 70 mg of the apo-myoglobin were dissolved in 60 mL of a 0.1 M phosphate buffer at pH = 7.5. The apo-protein solution was placed in a modified tonometer with a side tube that contained a few grains of sodium dithionite. The tube is connected to a second test tube containing 9 mg of Co(II)-protoporphyrin IX in 6 mL 50% aqueous pyridine. The solution was deoxygenated by a gentle flow of nitrogen which passed over the protein solution and bubbled into the porphyrin solution. After deoxygenation is completed, the Co(II)-protoporphyrin IX solution was forced into the side tube containing the dithionite, by reversing the gas flow. The reduced metalloporphyrin is mixed with the apo-myoglobin solution for 1 h. The resulting solution was dialyzed against 0.01 M phosphate buffer at pH = 7.5 (2 times against 1 L of the buffer, each dialysis was conducted for 6 h), and the resulting reconstituted protein was purified on Sephadex G-25 column equilibrated with 0.01 M phosphate buffer at pH = 7.5. The fraction of the Mb-Co(II) solution was lyophilized and the solid was stored at −18 °C.

Preparation of Eosin-Modified Mb-Co(II), Eo^{2-}-Mb-Co(II), and Eosin-Modified apo-Mb. To a freshly prepared solution of Co(II)-protoporphyrin IX-reconstituted myoglobin, Mb-Co(II), (70 mg) were added 10 mg of eosin-5-isothiocyanate (**3**). The pH of the system was adjusted to pH = 7.5 and the solution was stirred for 20 h, 4 °C. The resulting mixture was dialyzed twice against 1 L of phosphate buffer, 0.01 M, pH = 7.5, each time for 3 h. The dialyzed solution was further purified by gel-filtration on a 15 × 2 cm Sephadex-G10 column, using a phosphate buffer solution as eluent. The eosin-modified fraction of Eo^{2-}-Mb-Co(II) was identified spectroscopically. The eosin-modified apo-Mb was prepared by a similar method by reacting apo-Mb (70 mg) with eosin-5-isothiocyanate (10 mg).

Separation of α- and *β*-Hemoglobin Subunits. Separation of α- and *β*-Hb subunits was performed by slight modification of the method reported in the literature.[26] Hemoglobin (Bovine Hb), 1.0 g, was dissolved in 10 mL of water. To this solution were added 1 mL of a 0.2 M sodium dihydrogen phosphate solution and 0.15 mL of a saturated NaCl solution. *p*-Hydroxy mercury benzoate, 50 mg, was dissolved in a minimum volume of NaOH, 1 M, and 1 mL of water was added to the solution. To the resulting solution was slowly added a 1 M acetic acid solution until a slight turbidity appeared (pH = 9.5). The protein solution was rapidly added to the *p*-hydroxy mercury benzoate solution, and the pH of the resulting solution was adjusted to pH = 6.0 by the addition of 3 drops of acetic acid. The solution was stirred for 24 h, 4 °C. The precipitate formed in the system was removed with a centrifuge, and the clear solution was dialyzed against phosphate buffer, 0.01 M, pH = 6.2. The α-Hb subunit and the *p*-hydroxy mercury benzoate *β*-Hb subunit were separated by medium pressure chromatography over a 2 × 20 cm carboxymethyl Sephadex-CM25 column, using a gradient eluting solution. The separation of the fraction was visually observed by the formation of red-brown bands. The *p*-hydroxy mercury benzoate-protected *β*-Hb was eluted first using a phosphate buffer solution, 0.01 M, pH = 6.8 as eluent. By gradual increase of the eluent composition to 0.02 M Na_2HPO_4, a fraction of the native Hb was eluted. Further increase of the eluent concentration to 0.04 M Na_2HPO_4 resulted in the α-Hb fraction. The α-Hb protein and the *p*-hydroxy mercury benzoate-protected *β*-Hb were lyophilized to dryness. Deprotection of the *p*-hydroxy mercury benzoate *β*-Hb was accomplished by dissolving 100 mg of the protected *β*-Hb in 15 mL of phosphate buffer, 0.1 M, pH = 7.5. Mercaptoethanol, 50 μL, was added to the solution, and the system was stirred for 2 h at room temperature. The *β*-Hb was then purified by gel filtration over Sephadex-G10; the elution was performed with phosphate buffer 0.04 M. The complete deprotection was verified by determination of the mercury content in the resulting protein by atomic absorption. The resulting eluted solution of *β*-Hb was dialyzed three times against 1 L of water.

Preparation of apo-α- and -*β*-Hb. The method for the preparation of apo α- and *β*-Hb was identical to that described for apo-Mb. The differences were introduced in the final dialysis steps. Apo-*β*-Hb was dialyzed against a 0.025 M HEPES buffer solution, pH = 6.5, that included Na_2EDTA, 0.5 mM. These conditions are essential to preserve the cysteine residue in the reduced-SH state. The apo-α-Hb, lacking cysteine residues, was dialyzed against a 0.025 mM HEPES buffer solution, pH = 7.0.

Reconstitution of apo-α-Hb and apo-*β*-Hb with Co(II)-Protoporphyrin IX, α-Hb-Co(II) and *β*-Hb-Co(II). Reconstitution of apo α-Hb and apo *β*-Hb with Co(II)-protoporphyrin IX to generate α-Hb-Co(II) and *β*-Hb-Co(II) was performed directly on the apo-α-Hb and apo-*β*-Hb obtained after dialysis by the procedure described for Mb-Co(II). The crude α-Hb-Co(II) and *β*-Hb-Co(II) solutions were used for further modification with the chromophore. In order to have the purified reconstituted proteins, α-Hb-Co(II) and *β*-Hb-Co(II), the crude solutions were treated as described for Mb-Co(II).

Chemical Modification of α-Hb-Co(II) and *β*-Hb-Co(II) by the Eosin Chromophore. The crude solution of *β*-Hb-Co(II) obtained after reconstitution was adjusted to pH = 6.6 with several drops of HCl. Eosin-5-maleimide (**4**), 5 mg, was added to the solution that was further stirred for 30 min at room temperature. The resulting crude Eo^{2-}-*β*-Hb-Co(II) solution was dialyzed against a 0.01 M phosphate buffer solution, pH = 7.5, and further purified by gel-filtration over Sephadex-G25 using a phosphate buffer, 0.01 M, pH = 7.5, as eluent.

The crude solution of α-Hb-Co(II) obtained after reconstitution was adjusted to pH = 7.0 by the addition of several drops of HCl. Eosin-5-maleimide (**4**), 5 mg, was added to the solution that was stirred further for 30 min at room temperature. The crude Eo^{2-}-α-Hb-Co(II) solution was further purified by the method described for Eo^{2-}-*β*-Hb-Co(II). Apo-α-Hb and apo-*β*-Hb were modified by eosin-5-maleimide (**4**) by procedures identical to those described for the preparation and purification of Eo^{2-}-α-Hb-Co(II) and Eo^{2-}-*β*-Hb-Co(II), respectively.

Photocatalyzed H_2-Evolution and Hydrogenation of Acetylenes by Steady-State Irradiation of Eo^{2-}Mb-Co(II) or Eo^{2-}-α-Hb-Co(II) or Eo^{2-}-*β*-Hb-Co(II). A 0.1 M phosphate buffer solution, pH = 7.5, (3 mL) that included the photoenzyme Eo^{2-}-Mb-Co(II) (or Eo^{2-}-α-Hb-Co(II) or Eo^{2-}-*β*-Hb-Co(II)), 0.17 mg·mL^{-1}, and the sacrificial electron donor, Na_2EDTA, 0.01 M, was placed in a glass cuvette equipped with a micro magnetic stirrer and a rubber septum. For the H_2-evolution experiments, the cuvette was repeatedly evacuated and flushed with Ar. For the hydrogenation of acetylene the cuvette was evacuated and further saturated with acetylene by bubbling the gas (C_2H_2) for 5 min. In the system for the hydrogenation of acetylene-dicarboxylic acid, the substrate was added to the system (0.001, 0.0025, 0.005, and 0.01 M, respectively), and the cuvette was evacuated and flushed with Ar. The systems were irradiated with a 150 W-Xe arc lamp and filtered through an optical filter, $\lambda > 475$, and a $CuSO_4$ solution. H_2-evolution was analyzed by taking 500 μL gas samples at time intervals of illumination and gas chromatographic analysis on a MS 5 Å column (TCD, oven temperature 35 °C, argon carrier gas). Photohydrogenation of acetylene to ethylene was followed by taking out 100 μL samples of the gas at time intervals of irradiation and gas chromatographic analysis over a Poropak N column (FID, oven temperature 40 °C, N_2 carrier gas). Photohydrogenation of acetylene-dicarboxylic acid was followed by exclusion of 100 μL samples of the solution at time intervals of illumination. The samples were filtered through a RC-58 filter (Schlercher & Schuell) and Dowex 50Wx8 and

(26) (a) Bucci, E. In *Methods in Enzymology*; Antonini, E., Rossi-Bernardi, L., Chiancone, E., Eds.; Academic Press: London, 1981; Vol. 76, pp 97−106. (b) Antonini, E.; Brunori, M. *Hemoglobin and Myoglobin in Their Reaction with Ligand*; North-Holland Publishing Co.: Amsterdam, 1971; pp 9−12.

analyzed by HPLC using a Shodex KC-811 anion exchange column and a 0.25% H_3PO_4 solution as eluent (0.9 mL·min^{-1}). The detection of the eluted acid was spectroscopic, $\lambda = 218$ nm. Under these conditions, the retention times are as follows: acetylenedicarboxylic acid, 5.8 min; maleic acid, 7.6 min, and fumaric acid, 13 min.

The experiments in the reference systems included Mb-Co(II), 0.15 mg·mL^{-1} and eosin, Eo^{2-}, 2.5×10^{-5} M, or Co(II)-protoporphyrin IX, 1.23×10^{-5} M, and eosin, Eo^{2-} 2.5×10^{-5} M, respectively, where all other conditions were identical to those described for the Eo^{2-}-Mb-Co(II) system. These concentrations correspond to the concentration of each of the components in the Eo^{2-}-Mb-Co(II) photosystem.

Time-Resolved Studies in the Eo^{2-}-Mb-Co(II), Eo^{2-}-α-Hb-Co-(II), and Eo^{2-}-β-Hb-Co(II) Systems. A phosphate buffer solution, 0.1 M, pH = 7.5, that included the respective protein, 0.17 mg·mL^{-1}, was placed in a glass cuvette equipped with a rubber septum. The sacrificial electron donor, Na_2EDTA, was added in the appropriate experiments. The system was evacuated for 5 min and flushed with Ar for 10 min. The system was flashed ($\lambda = 532$ nm pulse width <5 ns; pulse energy 35 mJ/pulse), and the respective transients were recorded and analyzed.

Cyclic Photocatalyzed Hydrogenation of Acetylene by Lactic Acid under Steady-State Irradiation. A phosphate buffer solution, 0.1 M, pH = 7.5 that included Eo^{2-}-Mb-Co(II), 0.11 mg·mL^{-1}, *N*-methylferrocene caproic acid (**5**) 8×10^{-3} M, and L-lactic acid, 1.5×10^{-2} M, was placed in a glass cuvette equipped with a magnetic stirrer and a rubber septum. The system was evacuated and further saturated with acetylene by bubbling C_2H_2 through the solution. To the system were injected 400 μL of a lactate dehydrogenase, LDH, solution that included 13.6 mg of the protein, 1.8 units. The system was irradiated with a 150W Xe-arc lamp. The light was filtered through an optical filter, $\lambda > 475$ nm, and a $CuSO_4$ solution. Gas samples, 200 μL, and solution samples, 100 μL, were taken from the system at time intervals of illumination. The gas samples were analyzed by gas chromatography for ethylene (Poropak N column, FID). The solution samples were analyzed by HPLC using a Shodex KC-811 anion exchange column and a 0.1% H_3PO_4 solution as eluent (0.6 mL·min^{-1}, spectroscopic detection $\lambda = 210$ nm). The retention times corresponded to the following: pyruvic acid, 11.7 min, lactic acid 14.5 min.

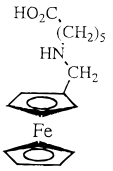

(5)

Redox Properties of Mb and Mb-Co(II). The proteins do not electrically communicate with electrodes. Special treatment of graphite electrodes enabled the adsorption of the proteins and the direct examination of their electrochemical features.[27] Didodecyl dimethylammonium bromide, DDAB, was sonicated in water for 24 h to generate a 0.01 M solution. A cylindrical graphite electrode was polished in the presence of the respective protein solution, 1.0 mg·mL^{-1} and the DDAB solution. The resulting modified electrode was introduced into the electrochemical cell that included a phosphate buffer solution, 0.1 M, pH = 7.5, as electrolyte, a counter Pt electrode and SCE as reference electrode. Cyclic voltammograms were recorded under Ar, scan-rate 50 mV·s^{-1}.

Results and Discussion

The concept to generate semisynthetic photoenzymes is based on the reconstitution of the native hemoproteins, myoglobin, Mb, and α- or β-hemoglobin subunits, α-Hb or β-Hb. The method of reconstitution is schematically outlined in Figure 1. The native protoheme (**1**) site was excluded from the native proteins, and the respective apo-proteins were reconstituted with

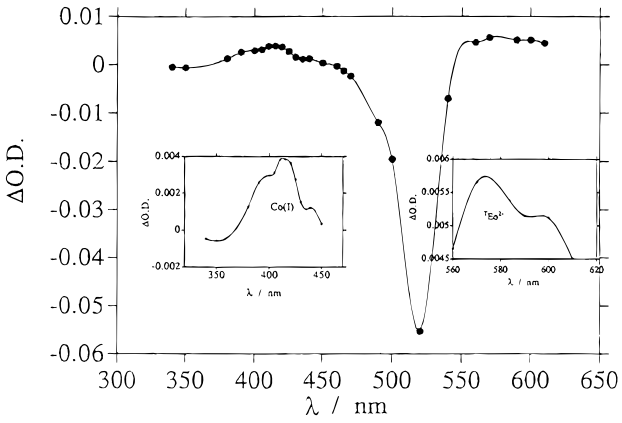

Figure 3. Transient absorption spectra upon excitation of Eo^{2-}-Mb-Co(II) (0.17 mg/mL) in 0.1 M phosphate buffer, pH = 7.5. The spectra were recorded 0.1 μs after the excitation pulse (532 nm).

Co(II)-protoporphyrin IX (**2**). The Co(II)-reconstituted myoglobin, Co(II)-Mb, or hemoglobin subunits, Co(II)-α-Hb or Co(II)-β-Hb, respectively, were then modified with an eosin chromophore to yield the photoactive protein assembly. The reconstitution of native myoglobin, or hemoglobin, by metal-protoporphyrin IX complexes was previously used in studying photoinduced electron transfer in proteins.[6,22] In our study, the Co(II)-porphyrin site was included in the reconstituted proteins since it acts as an electron-acceptor site for excited chromophores and simultaneously, the photoreduced Co(I)-species is capable of generating cobalt-hydride species which catalyze various chemical transformations such as hydrogenation or CO_2-fixation.[28] The eosin chromophore, as other xanthene dyes, was previously employed to photostimulate electron transfer reactions.[29]

Photoinduced Electron Transfer in Eosin-Modified Co(II)-Reconstituted Myoglobin, Eo^{2-}-Mb-Co(II). apo-Myoglobin was reconstituted with Co(II)-protoporphyrin IX, (**2**), as outlined in Figure 1. The absorption spectrum of the reconstituted Mb-Co(II) shows an absorbance at $\lambda = 426$ nm characteristic to the Co(II)-protoporphyrin chromophore. From the absorbance at $\lambda = 426$ nm ($\epsilon = 140\,000$ M^{-1}·cm^{-1})[30] of a known protein sample the ratio of Co(II)-porphyrin to protein was estimated to be 1:1. The reconstituted Mb-Co(II) was reacted with eosin isothiocyanate (**3**) to yield the chromophore-modified protein, Eo^{2-}-Mb-Co(II), eq 1. The absorption spectrum of Eo^{2-}-Mb-Co(II) includes, in addition to the Co(II)-porphyrin absorbance band at $\lambda = 426$ nm, the characteristic absorbance band of the eosin chromophore at $\lambda = 524$ nm. From the extinction coefficient of the eosin chromophore (ϵ(524 nm) = 83 000 M^{-1}·cm^{-1}),[23] the average loading was calculated to correspond to two eosin units per protein molecule.

The photoinduced electron transfer reactions in the Eo^{2-}-Mb-Co(II) assembly were characterized by laser flash photolysis. Figure 3 shows the transient spectrum of the system formed upon excitation of the eosin chromophore. The bleaching of

(27) (a) Rusling, J. F.; Nassar, A. F. *J. Am. Chem. Soc.* **1993**, *115*, 11891−11897. (b) Nassar, A. F.; Willis, W. S.; Rusling, J. F. *Anal. Chem.* **1995**, *67*, 2386−2392.

(28) (a) Tinnemans, A. H. A.; Koster, T. P. M.; Thewissen, D. H. M. W.; Mackor, A. *Recl. Trav. Chim. Pays-Bas* **1984**, *103*, 282−295. (b) Creutz, C.; Sutin, N. *Coord. Chem. Rev.* **1985**, *64*, 321−341. (c) Darensbourg, D. J.; Kudaroski, R. A. In *Advances in Organometallic Chemistry*; Stone, F. G. A., West, R., Eds.; Academic Press: New York, 1983; Vol. 22, pp 129−168.

(29) (a) Willner, I.; Eichen, Y.; Joselevich, E.; Frank, A. J. *J. Phys. Chem.* **1992**, *96*, 6061−6066. (b) Joselevich, E.; Willner, I. *J. Phys. Chem.* **1994**, *98*, 7628−7635. (c) Joselevich, E.; Willner, I. *J. Phys. Chem.* **1995**, *99*, 6903−6912. (d) Neckers, D. C.; Valdes-Aguilera, O. M. In *Advances in Photochemistry*; Volman, D., Hammond, G. S., Neckers, D. C., Eds.; John Wiley & Sons, Inc.: New York, 1993; Vol. 18, pp 315−394.

(30) Yonetani, T.; Yamamoto, H.; Woodrow, G. V., III. *J. Biol. Chem.* **1974**, *249*, 682−690.

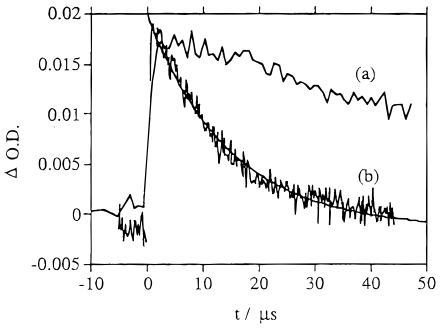

Figure 4. Transient decay of the photogenerated eosin triplet (followed at 590 nm) of (a) Eo^{2-}-apo-Mb and (b) $^{T}Eo^{2-}$-Mb-Co(II).

the ground-state is observed at $\lambda = 524$ nm, the absorbance of the $^{T}Eo^{2-}$-Mb-Co(II) is detected at $\lambda = 590$ nm, and, in addition, a transient absorbance at $\lambda = 406$ nm characteristic to the Co(I)-protoporphyrin is detected. This indicates that excitation of the eosin chromophore results in its oxidative quenching via electron transfer, eq 2. Since the eosin-triplet lifetime is

$$^{T}Eo^{2-}\text{-Mb-Co(II)} \xrightarrow{k_q = 6.3 \times 10^4\ s^{-1}} Eo^{\bullet -}\text{-Mb-Co(I)} \quad (2)$$

sensitive to its chemical environment, and, in order to quantitatively determine the electron-transfer quenching rate constant, k_q, the eosin chromophore was linked to apo-Mb that lacks the Co(II)-acceptor site. Figure 4 shows the eosin-triplet decay of $^{T}Eo^{2-}$-apo-Mb (curve a) and $^{T}Eo^{2-}$-Mb-Co(II) (curve b). Both curves fit single-exponential decays, and from the shortening of the lifetime in $^{T}Eo^{2-}$-Mb-Co(II) as compared to the reference compound, the electron transfer quenching rate constant was estimated to be $k_q = 6.3 \times 10^4\ s^{-1}$. Note, however, that the lifetime of the eosin-triplet in $^{T}Eo^{2-}$-apo-Mb, 71 μs, is particularly short as compared to the characteristic lifetimes of eosin. This aspect will be considered later. The quenching process of $^{T}Eo^{2-}$-Mb-Co(II) proceeds via electron transfer, eq 2. This is evident from the formation of the Co(I)-protoporphyrin IX site followed at $\lambda = 400$ nm. Figure 5(A) shows the transient decay of the Co(I) species as a result of the back-electron transfer, eq 3. The decay is single-exponential and the back electron-transfer rate constant corresponds to $k_{bq} =$

$$Eo^{\bullet -}\text{-Mb-Co(I)} \xrightarrow{k_{bq} = 1.4 \times 10^5\ s^{-1}} Eo^{2-}\text{-Mb-Co(II)} \quad (3)$$

$1.4 \times 10^5\ s^{-1}$. The kinetics of restoration of the ground-state system, Eo^{2-}-Mb-Co(II), can be analyzed by following the recovery of the bleached chromophore at $\lambda = 510$ nm, Figure 5(B). The transient of the recovery of the bleached chromophore does not fit a monoexponential kinetics, but fits a biexponential process, where one population (70%) recovers at a rate constant of $1.4 \times 10^5\ s^{-1}$, and the second population (30%) restores the ground-state at a slower rate constant, $k = 3.5 \times 10^4\ s^{-1}$. The population that resotres the ground-state at the fast kinetics, $k = 1.4 \times 10^5\ s^{-1}$ (70%) corresponds to the back electron transfer of the photogenerated redox species, eq 3. The second population that recovers the ground state cannot be the decay of the unquenched triplet $^{T}Eo^{2-}$-Mb-Co(II), since it decays at a substantially longer time scale (vide infra).

To account for the second population of the species recovering the ground-state, Eo^{2-}-Mb-Co(II), we should note that the eosin-modified reconstituted Mb-Co(II) is loaded with two chromophore units. Previous studies[21,31] have indicated that in proteins, i.e., glutathione reductase, that includes two eosin chromophore units, a self-quenching mechanism is operative. Also, the lifetime of the eosin chromophore in Eo^{2-}-apo-Mb is substantially shorter (71 μs) than the lifetime of an isolated eosin unit (1850 μs). These observations suggest that the two eosin units attached to the reconstituted myoglobin undergo a self-quenching process, eq 4. If this electron transfer quenching route is indeed operative, recombination of the photogenerated redox species, eq 5, could account for the second population that restores the ground-state. To support this mechanism the

$$(^{T}Eo^{2-} + Eo^{2-})\text{-Mb-Co(II)} \xrightarrow{k_{sq} = 1.4 \times 10^4\ s^{-1}} (Eo^{\bullet 3-} + Eo^{\bullet -})\text{-Mb-Co(II)} \quad (4)$$

$$(Eo^{\bullet 3-} + Eo^{\bullet -})\text{-Mb-Co(II)} \xrightarrow{k_{bsq} = 3.5 \times 10^4\ s^{-1}} (Eo^{2-} + Eo^{2-})\text{-Mb-Co(II)} \quad (5)$$

eosin-modified apo-Mb (loaded with two chromophore units) was examined by laser flash photolysis. Figure 6 shows the transient absorption spectrum obtained upon excitation of this system. In addition to the bleaching of the ground-state, $\lambda =$ 520 nm, and formation of the eosin triplet, $\lambda = 590$ nm, the absorption bands characteristic of $Eo^{\bullet -}$, $\lambda = 410$ nm, and $Eo^{\bullet 3-}$, $\lambda = 440$ nm, are observed. These results clearly indicate that the self-quenching route is indeed operative in Eo^{2-}-apo-Mb. By comparing the lifetime of the chromophore in $^{T}Eo^{2-}$-apo-Mb with that of an isolated chromophore (1850 μs),[31] the self-quenching rate constant was calculated to be $k_{sq} = 1.4 \times 10^4\ s^{-1}$. The transients of the $Eo^{\bullet 3-}$ and $Eo^{\bullet -}$ species formed upon photoexcitation of Eo^{2-}-apo-Mb, decay monoexponentially with similar rate constants, $k_{bsq} = 3.5 \times 10^4\ s^{-1}$. Note that this rate constant is similar to the decay constant observed for the second population that resotres Eo^{2-}-Mb-Co(II), suggesting that the second population restoring the ground-state, Eo^{2-}-Mb-Co(II), originates from the recombination of the redox species formed by the self-quenching route, eq 5. Further support that the self-quenching route of the chromophore occurs in Eo^{2-}-Mb-Co(II), and that the second population that resotres the ground-state corresponds to species formed by this route, is obtained by calculating the quantum yields of the two populations using the two quenching rate constants, k_q and k_{sq}. The quantum yields of the photoproducts, $Eo^{\bullet -}$-Mb-Co(I), $\phi_q = k_q/(k_{sq} + k_q)$, and of $(Eo^{3-} - Eo^{\bullet -})$-Mb-Co(II), $\phi_{sq} = k_{sq}/(k_{sq} + k_q)$, are derived by substitution of the respective quenching rate-constants. The derived values, $\phi_q = 0.8$ and $\phi_{sq} = 0.2$ are similar to the population of different species determined by the biexponential analysis of the recovery of the bleached species, Figure 5(B).

The oxidative electron-transfer quenching of Eo^{2-}-Mb-Co(II) leads to the photoproduct $Eo^{\bullet -}$-Mb-Co(I). To overcome the back electron transfer, and to allow the further utilization of the reduced photoproduct in photosynthetic transformations, the sacrificial electron donor, Na_2EDTA was added to the system. Figure 7(A) shows the transient of the Co(I) species observed upon excitation of the Eo^{2-}-Mb-Co(II) in the absence (curve a) and presence (curve b) of Na_2EDTA. Figure 7(B) shows the transient recovery of the bleached ground-state Eo^{2-}-chromophore. In the absence of Na_2EDTA the Co(I) species decays by the back electron transfer, eq 3, while in the presence of Na_2EDTA, the Co(I) species is accumulated in the system due to the oxidation of the sacrificial electron donor, eq 6. The ground-state Eo^{2-}-chromophore is recovered by a rapid bimolecular rate constant, $k_{ox} = 2 \times 10^7\ M^{-1}\cdot s^{-1}$ that corresponds to the oxidation of Na_2EDTA by the oxidized intermediate, eq 6, and then by a slow process $k_r = 330 \pm 20\ s^{-1}$. The Co(I)

(31) Kasche, V.; Lindqvist, L. *Photochem. Photobiol.* **1965**, *4*, 923–933.

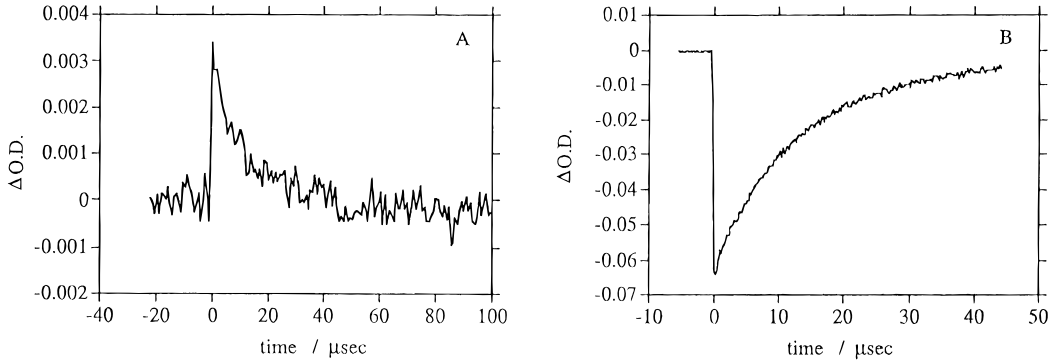

Figure 5. (A) Transient decay of the photogenerated Co(I) in the redox assembly $Eo^{\bullet -}$-Mb-Co(I) (followed at 400 nm). (B) Transient recovery of the eosin ground state of Eo^{2-}-Mb-Co(II) (followed at $\lambda = 510$ nm).

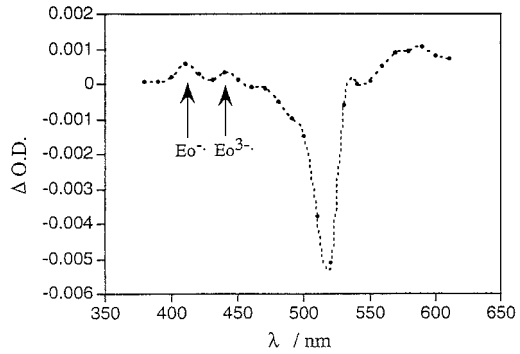

Figure 6. Transient absorption spectrum formed upon excitation of Eo^{2-}-apo-Mb (0.17 mg/mL^{-1}) in 0.1 phosphate buffer, pH = 7.5. The spectrum was recorded 0.1 μs after the excitation pulse (532 nm).

species is formed by a rapid process with a first-order rate

$$Eo^{\bullet -}\text{-Mb-Co(I)} + Na_2EDTA \xrightarrow{k_{ox} = 2 \times 10^7\ M^{-1}\cdot s^{-1}} Eo^{2-}\text{-Mb-Co(I)} + Na_2EDTA_{ox}$$

$$\downarrow$$

$$\text{decomposition products} \quad (6)$$

constant of $k_q = 5.2 \times 10^4\ s^{-1}$ and then by a process that exhibits a substantially slower time-constant ($k_r = 330 \pm 20\ s^{-1}$). The slow component leading to the formation of Co(I) and to the slow recovery of the ground-state chromophore, originates from the slow reduction of the Co(II)-center by the $Eo^{\bullet 3-}$ species formed by the dye self-quenching route and is accumulated in the presence of the sacrificial electron donor, eq 7 and eq 8.[32] Scheme 1 summarizes the two paths of photoinduced electron transfer in Eo^{2-}-Mb-Co(II).

We have examined the photophysics of two additional reference systems. One includes Mb-Co(II) and diffusional

$$(Eo^{\bullet 3-} + Eo^{\bullet -})\text{-Mb-Co(II)} + Na_2EDTA \xrightarrow{k_{ox} = 2 \times 10^7\ M^{-1}\cdot s^{-1}} (Eo^{\bullet 3-} + Eo^{2-})\text{-Mb-Co(II)} + Na_2EDTA_{ox}$$

$$\downarrow$$

$$\text{decomposition products} \quad (7)$$

$$(Eo^{\bullet 3-} + Eo^{2-})\text{-Mb-Co(II)} \xrightarrow{k_r = 330 \pm 20\ s^{-1}} Eo^{2-}\text{-Mb-Co(I)} \quad (8)$$

eosin as chromophore and the second system that includes the diffusional components Eo^{2-} and Co(II)-protoporphyrin IX without the protein. The deduced electron-transfer quenching rate constants are given in eq 9 and eq 10. The quenching

$$^{T}Eo^{2-} + \text{Mb-Co(II)} \xrightarrow{k_q = 2.5 \times 10^3\ M^{-1}\cdot s^{-1}} Eo^{\bullet -} + \text{Mb-Co(I)} \quad (9)$$

$$^{T}Eo^{2-} + \text{Co(II)-PorIX} \xrightarrow{k_q = 1.9 \times 10^9\ M^{-1}\cdot s^{-1}} Eo^{\bullet -} + \text{Co(I)-PorIX} \quad (10)$$

$$Eo^{\bullet -} + \text{Mb-Co(I)} \xrightarrow{k_{bM} = 1.5 \times 10^9\ M^{-1}\cdot s^{-1}} Eo^{2-} + \text{Mb-Co(II)} \quad (11)$$

$$Eo^{\bullet -} + \text{Co(I)-PorIX} \xrightarrow{k_{bP} = 1.8 \times 10^{12}\ M^{-1}\cdot s^{-1}} Eo^{2-} + \text{Co(II)-PorIX} \quad (12)$$

efficiency in the system that includes Eo^{2-} and Mb-Co(II) is substantially lower than the quenching rate in the Eo^{2-}-Mb-Co(II) assembly. This is due to the inefficient electrical contact between the diffusional excited chromophore, $^{T}Eo^{2-}$, and the electron acceptor embedded in the protein matrix. The back electron transfer rate-constants of the generated redox species

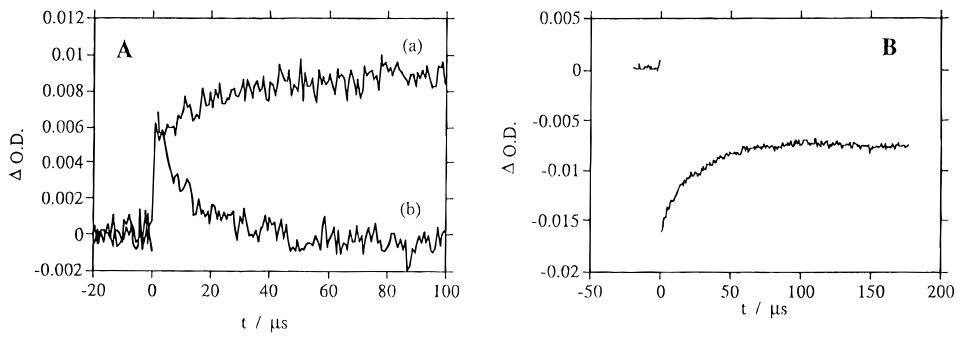

Figure 7. (A) Transients of Co(I) species formed upon photoexcitation of Eo^{2-}-Mb-Co(II) (followed at $\lambda = 400$ nm): (a) in the absence of Na_2EDTA and (b) in the presence of Na_2EDTA, 0.01 M. (B) Transient restoration of eosin ground state of Eo^{2-}-Mb-Co(II) followed at 510 nm in the presence of Na_2EDTA, 0.01 M.

Scheme 1. Electron Transfer Pathways upon Photoexcitation of Eo^{2-}-Mb-Co(II)

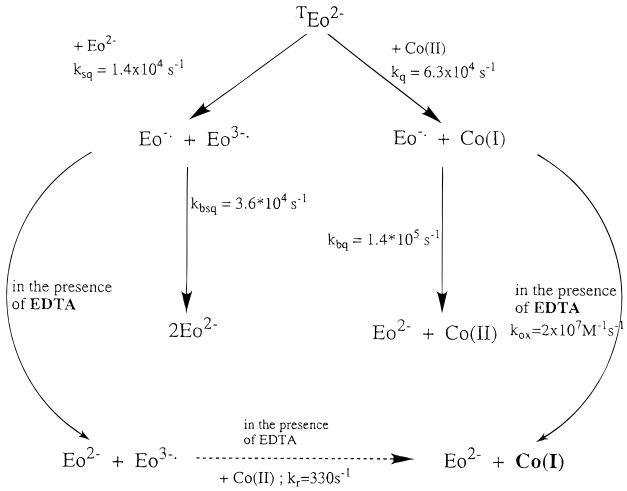

in the two reference systems are summarized in eq 11 and eq 12. The back electron transfer rate in the system that includes eosin and Co(II)-protoporphyrin, without the protein matrix, is very fast. Thus, the photosystem, Eo^{2-}-Mb-Co(II) reveals superior functions as compared to the two reference systems. It shows effective electron transfer quenching and a reasonably long lifetime of the photogenerated redox species due to the association of the chromophore and Co(II)-center with the protein. The covalent linkage of the chromophore to the protein facilitates the quenching process, but simultaneously, the separation of the redox species by the protein stabilizes the photoproducts against back electron transfer. These aspects will be important in analyzing the photocatalytic features of Eo^{2-}-Mb-Co(II) and those of the reference systems.

Photocatalytic Transformations in the Presence of Eo^{2-}-Mb-Co(II). The characterization of the photoinduced electron transfer reactions in Eo^{2-}-Mb-Co(II) indicated that oxidative quenching of the chromophore yields the Co(I)-photoproduct and that in the presence of the sacrificial electron donor, Na_2-EDTA, the Eo^{2-}-Mb-Co(I) is accumulated. The reduced Co(I) center in a protic medium such as water, forms a Co(III)-H species. Formation of the Co(III)-H species could then be an efficient catalytic species for various chemical transformations, i.e., hydrogen evolution by protonation or hydrogenation of unsaturated compounds or CO_2 via insertion of the respective substrates.[28]

Steady-state irradiation, $\lambda = 475$ nm, of an aqueous solution, pH = 7.5, of Eo^{2-}-Mb-Co(II) in the presence of Na_2EDTA yields the evolution of hydrogen. The quantum yield of H_2-evolution corresponds to $\phi = 2 \times 10^{-4}$. Control experiments revealed that irradiation of Mb-Co(II) in the presence of Na_2-EDTA or of Eo^{2-}-apo-Mb and Na_2EDTA does not yield any H_2-evolution. These experiments indicate that the eosin chromophore as well as the Co(II)-protoporphyrin IX center are essential components for H_2-evolution. Similarly, irradiation of Eo^{2-}-Mb-Co(II) in the absence of Na_2EDTA, does not produce hydrogen, indicating that the sacrificial electron donor is an essential ingredient.

The evolution of hydrogen is attributed to the protonation of the Co(III)-H intermediate formed via the Co(I) species generated by the photoinduced electron transfer, eq 13. Nonetheless, the quantum yield for H_2-evolution is very low as compared to

$$\text{Co(I)} + \text{H}^+ \rightarrow \text{Co(III)} - \text{H} \xrightarrow{\text{H}^+} \text{Co(III)} + \text{H}_2 \quad (13)$$

the quantum yield for the formation of the Co(I)-species in the photoinduced electron transfer, $\phi = 1.4 \times 10^{-2}$. Also, during irradiation of the photosystem, the protein exists in the reduced state, Eo^{2-}-Mb-Co(III)-H (characteristic absorbance, $\lambda_{max} = 406$ nm). These results suggest that the protonation of the Co(III)-H species is the slow, rate-limiting, process in H_2-evolution.

The fact that protonation of the Co(III)-H species is slow suggests that rapid insertion of appropriate substrates into the Co(III)-H could be used to drive the effective hydrogenation of the respective substrates with the concomitant inhibition of H_2-evolution. Steady-state irradiation of an aqueous photosystem, pH = 7.5, that includes Eo^{2-}-Mb-Co(II) and Na_2EDTA, and saturated with a gaseous atmosphere of acetylene results in the formation of ethylene. Under these conditions, H_2-evolution is blocked and ethylene is the only photoproduct. Figure 8 (curve a) shows the rate of ethylene formation at time intervals of illumination. The quantum yield for the ethylene production is $\phi = 1 \times 10^{-2}$. For comparison, the rates of ethylene formation in the two reference photosystems, consisting of Mb-Co(II) and diffusional Eo^{2-} (curve b), and of diffusional Eo^{2-} and Co(II)-protoporphyrin IX (curve c) are also shown. The efficiency of C_2H_4 formation in the two reference systems is substantially lower than in the presence of the chromophore-modified Co(II)-reconstituted myoglobin, Eo^{2-}-Mb-Co(II).

Formation of ethylene in the photosystem that includes Eo^{2-}-Mb-Co(II) and acetylene is attributed to the insertion of acetylene into the photogenerated Co(III)-H species, eq 14. It is interesting to note that the quantum yield for C_2H_4 formation is 50-fold higher than that for H_2-evolution in the analogous

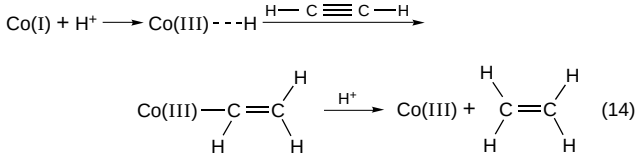

(14)

photosystem that lacks acetylene. This observation further supports the conclusion that protonation of the Co(III)-H intermediate is rate-limiting for H_2-evolution and explains the origin for the inhibition of H_2-evolution in the Eo^{2-}-Mb-Co(II) in the presence of C_2H_2. Insertion of acetylene into the Co(III)-H intermediate is faster than protonation leading to the selective photohydrogenation of acetylene to C_2H_4. The participation of the Co(III)-H species in H_2-evolution and hydrogenation of acetylene are further supported by kinetic isotope effects corresponding to 2.9 and 2.5 for the two transformations, respectively.

Figure 8 compares the rate of C_2H_4 formation in the photosystem Eo^{2-}-Mb-Co(II) to the two reference systems that include diffusional Eo^{2-} and Mb-Co(II) and the protein lacking photosystem that includes diffusional Eo^{2-} and Co(II)-protoporphyrin IX components. The efficiency of C_2H_4 formation in the reference photosystems is substantially lower than in the Eo^{2-}-Mb-Co(II) assembly. The low efficiency of C_2H_4 formation in the Mb-Co(II) and diffusional Eo^{2-} is attributed to the inefficient quenching of $^{T}Eo^{2-}$ by the Co(II)-center embedded in the protein. The low yield of ethylene formation in the photosystem that includes the diffusional Co(II)-protoporphyrin and Eo^{2-} is rationalized in terms of the rapid back-electron transfer reaction of the intermediate photoproducts. Thus, Eo^{2-}-Mb-Co(II) represents an assembly with the appropriate balance to stimulate the effective oxidative quenching of the excited chromophore due to its covalent attachment to the protein and

(32) The rate constant for the oxidation of Na_2EDTA by the $Eo^{\bullet -}$ species was also determined by following the depletion of $Eo^{\bullet -}$ or the accumulation of $Eo^{\bullet 3-}$ in the reference system ($Eo^{\bullet 3-}$-$Eo^{\bullet -}$)-apo-Mb in the presence of Na_2EDTA.

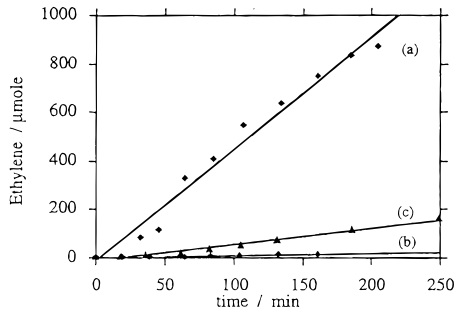

Figure 8. Rate of ethylene evolution at time intervals of illumination (λ > 475 nm) of (a) Eo^{2-}-Mb-Co(II), 0.17 mg·mL^{-1}, (b) Mb-Co(II), 0.17 mg·mL^{-1} and Eo^{2-}, 25 μM, (c) Co(II)-protoporphyrin IX, 12.3 μM and Eo^{2-}, 2.5 μM. In all systems Na_2EDTA, 0.01 M is included. All experiments were performed in 3 mL phosphate buffer, pH = 7.5, under saturated atmosphere of acetylene.

simultaneously to sufficiently stabilize the intermediate photoproducts by their spatial isolation via the protein matrix. Stabilization of the photoproducts against back electron transfer facilitates the reduction of the oxidized chromophore by the sacrificial electron donor and enables the effective formation of Eo^{2-}-Mb-Co(I) that acts as the catalyst for hydrogenation of ethylene.

Reconstitution of apo-Mb with Co(II)-protoporphyrin IX yields a catalytic active site in the protein for hydrogenation of acetylene. Thus, the Co(II)-reconstituted protein represents a semisynthetic biocatalyst. We were able to show that the reconstituted protein reveals features that mimic functions of natural enzymes. The kinetics of photohydrogenation of an acetylenic substrate was examined by following the rate of hydrogenation of acetylenedicarboxylic acid (**6**) in the photosystem Eo^{2-}-Mb-Co(II) and Na_2EDTA at different concentrations of **6**. The analysis was performed with the substrate (**6**) rather than with gaseous acetylene since it enables us to control precisely the concentration of the substrate in the aqueous medium. The photohydrogenation products of **6** are maleic acid

$$HO_2C{-}C{\equiv}C{-}CO_2H$$
(6)

(92%) and fumaric acid (8%). Figure 9(A) shows the initial rates of the formation of maleic acid (**7**) upon photohydrogenation of **6** by Eo^{2-}-Mb-Co(II), at different concentrations of **6**. The rate of maleic acid formation increases as the concentration of **6** increases. The maximum rate of hydrogenation of **6** is observed at a concentration of ca. 1×10^{-2} M and further

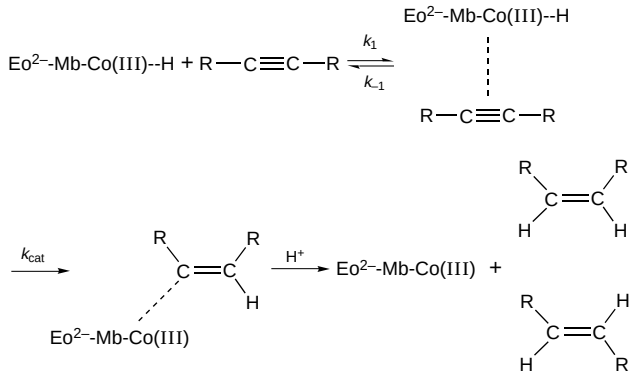

(15)

increase of the substrate concentration does not affect the hydrogenation rate. Assuming that the Co(II)-site in the reconstituted Eo^{2-}-Mb-Co(II) acts as active site for hydrogenation of **6**, eq 15, then the kinetics of hydrogenation of acetylenedicarboxylic acid (**6**) should follow the Michaelis−

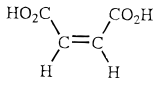

(7)

Menten model, eq 16, where V_o is the initial rate at any substrate concentration, V_{max} is the maximum rate upon saturation of the active-site by the substrate, and K_m is given by eq 17. The

$$\frac{1}{V_o} = \frac{1}{V_{max}} + \frac{K_m}{V_{max}}\frac{1}{[S]} \tag{16}$$

$$K_m = \frac{k_{cat}}{k_1 + k_{-1}} \tag{17}$$

experimental rates for photohydrogenation of **6** by Eo^{2-}-Mb-Co(II) at different concentrations of **6**, Figure 9(A), were analyzed according to eq 16, Figure 9(B). A linear relationship is obtained from which the values V_{max} = 0.6 μM·min^{-1} and K_m = 4 mM were derived. Thus, the semisynthetic protein assembly, Eo^{2-}-Mb-Co(II) follows the Michaelis−Menten model characteristic to enzymes.

Preparation of Photoenzymes by reconstitution of α- and *β*-Subunits of Hemoglobin. Preparation of the chromophore-modified Co(II) reconstituted myoglobin, Eo^{2-}-Mb-Co(II) revealed photoinduced electron transfer between the photoenzyme

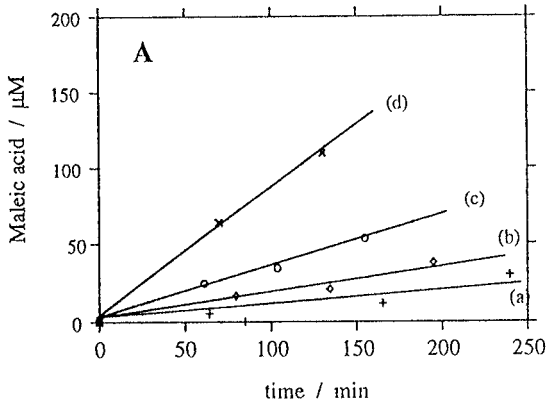

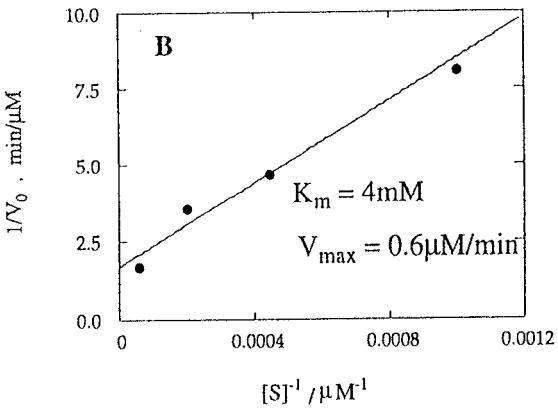

Figure 9. Photohydrogenation (λ > 475 nm) of acetylenedicarboxylic acid, (**6**), to maleic acid in a system composed of Eo^{2-}-Mb-Co(II), 0.17 mg·mL^{-1} in 3 mL 0.1 M phosphate buffer, pH = 7.5, that contains 0.01 M Na_2EDTA. (A) Initial rates of the maleic acid formation at different initial concentrations of **6**: (a) 1×10^{-3} M; (b) 2.5×10^{-3} M, (c) 5×10^{-3} M, and (d) 1×10^{-2} M. (B) Analysis of the hydrogenation rates of **6** to maleic acid according to eq 16: Lineweaver−Burk plot.

units. The system Eo^{2-}-Mb-Co(II) reveals, however, several scientific disadvantages. The modification sites of the protein by the Eo^{2-}-chromophore are unknown and hence the resulting photoenzyme lacks a defined structure. Also, the polysubstitution of the protein by two eosin units introduced a competitive self-quenching electron transfer pathway which complicated the electron transfer reactions in the resulting photoenzyme. A major advance could be accomplished by tailoring Co(II)-reconstituted photoenzymes that include a single eosin chromophore unit in defined structures. In such photoenzymes, the electron transfer parameters could be correlated with the protein structure and the self-quenching electron transfer route could be eliminated. Tailoring of site-specific eosin-modified Co(II)-reconstituted photoenzymes was based on the reconstitution of hemoglobin subunits (bovine source). Hemoglobin, Hb, is a tetramer of two identical α- subunits and two β-subunits. Each of the subunits includes a protoheme active center for oxygen binding. The separated subunits can function independently in binding of oxygen.

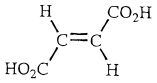

(**8**)

The Hb tetramer was separated to the α and β subunits by protection of the cysteine residues with *p*-hydroxymercury benzoic acid followed by chromatographic separation and removal of the protective group. The α or β-Hb heme subunits were reconstituted by the general method presented in Figure 1. The heme site was removed and the resulting apo-α-Hb and apo-β-Hb were reconstituted with Co(II)-protoporphyrin IX to yield α-Hb-Co(II) and β-Hb-Co(II). By analyzing the absorption bands at $\lambda = 426$ nm ($\epsilon = 120\,000$ $M^{-1}\cdot cm^{-1}$)[30] of samples of known protein content of α-Hb-Co(II) and β-Hb-Co(II), the loading of the reconstituted protein corresponds to 1:1.

The reconstituted α-Hb-Co(II) and β-Hb-Co(II) were further modified by the eosin chromophore. β-Hb-Co(II) includes a single cysteine 93 residue. The β-Hb-Co(II) was reacted at pH = 6.5 with eosin-4-maleimide (**4**), eq 18. At this pH value, lysine residues of the protein are protonated and Michael addition of cysteine to the maleimide residue is favored.[33] Figure 10(B) shows the absorption spectrum of Eo^{2-}-β-Hb-Co(II). The two absorption bands at $\lambda = 526$ nm ($\epsilon = 83\,000$ $M^{-1}\cdot cm^{-1}$) and $\lambda = 426$ nm ($\epsilon = 120\,000$ $M^{-1}\cdot cm^{-1}$) correspond to the eosin and Co(II)-protoporphyrin, respectively. The loading of eosin corresponds to 1. That is, Eo^{2-}-β-Hb-Co(II) is specifically modified at Cysteine-93 site by the eosin chromophore.[34]

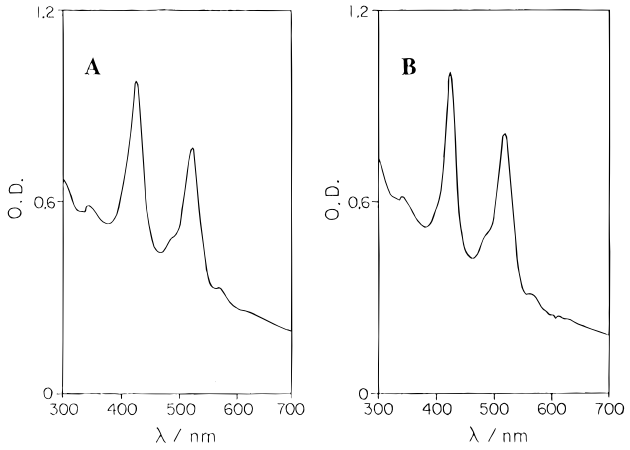

Figure 10. Absorption spectra of (A) Eo^{2-}-α-Hb-Co(II), 7 μM and (B) Eo^{2-}-β-Hb-Co(II), 7 μM.

The α-Hb-Co(II) reconstituted subunit does not include cysteine residues. Nevertheless, reaction of proteins with eosin-4-maleimide, (**4**), at pH > 7.0, where lysine residues are deprotonated, permits the Michael addition of amine groups to the maleimide site.[33] The α-Hb-Co(II) was reacted with (**4**) at pH = 7.0, at 4 °C, for 30 min to yield the eosin-modified Co(II)-reconstituted α-Hb, Eo^{2-}-α-Hb-Co(II), eq 19. Figure 10(A) shows the absorption spectrum of the resulting Eo^{2-}-α-

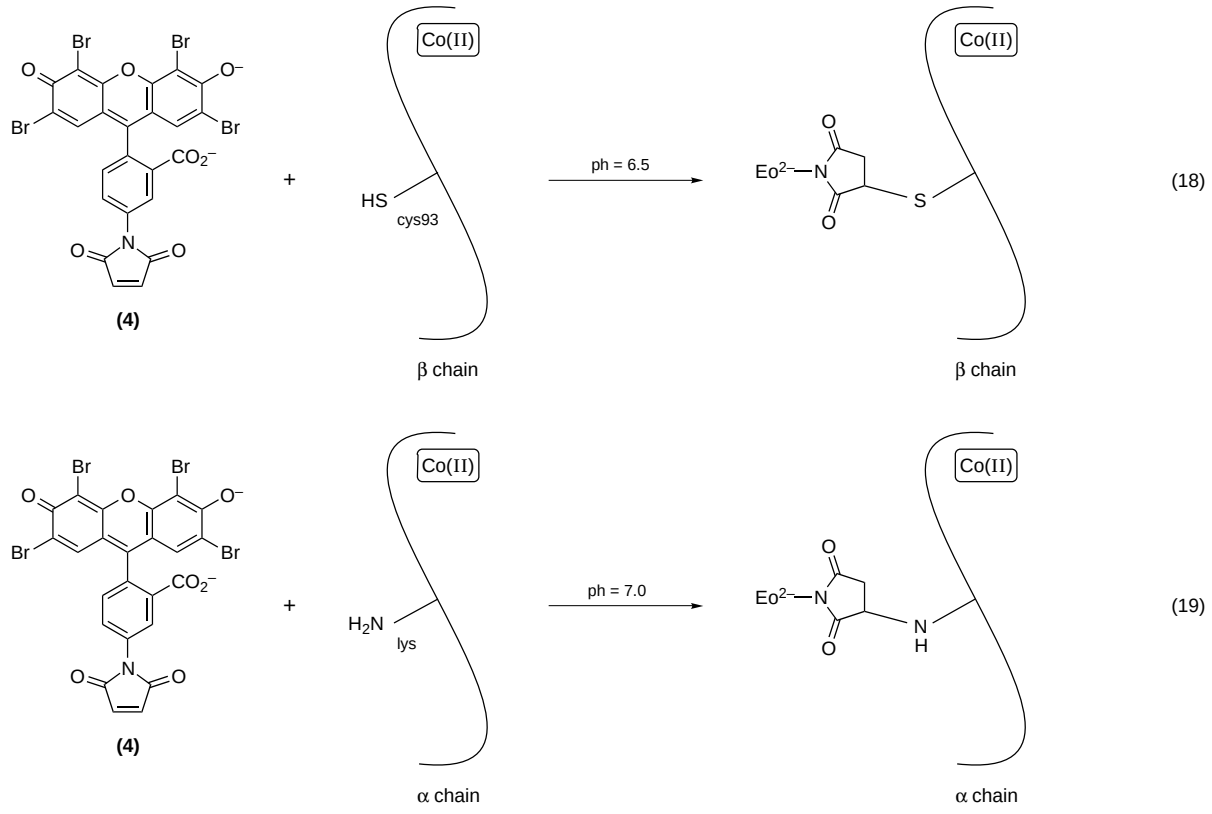

Hb-Co(II). The absorption bands at $\lambda = 526$ nm and $\lambda = 426$ nm correspond to the eosin and Co(II)-protoporphyrin units, respectively. From the absorbance of the two bands the molar ratio of eosin to Co(II) units is calculated to be 1:1. The α-Hb-Co(II) protein includes 11 lysine residues. The eosin loading of the resulting protein could correspond to an average loading and imply the presence of poly-substituted α-Hb-Co(II) residues by Eo^{2-}, or alternatively, single modification of different lysine sites by the eosin chromophore. Nonetheless, it was pointed out that poly-substitution of the protein by the eosin chromophore is accompanied by the self-quenching electron transfer path. It will be addressed later that no self-quenching electron transfer route is operative in Eo^{2-}-α-Hb-Co(II). It will also be shown that the eosin chromophore in Eo^{2-}-α-Hb-Co(II) reveals a single-exponential decay implying a single population of the chromophore. These observations suggest that Eo^{2-}-α-Hb-Co-(II) represents a protein assembly where a specific lysine residue is modified by a single Eo^{2-}-chromophore unit. The method to elucidate the modification site will be discussed later. We believe that the special conditions employed in the modification of α-Hb-Co(II), eq 19 (short reaction time and low temperature), and the availability of a single lysine residue exposed to the aqueous environment led to the site-specific formation of Eo^{2-}-α-Hb-Co(II).

Photoinduced Electron Transfer in Eo^{2-}-α-Hb-Co(II) and Eo^{2-}-*β*-Hb-Co(II). The photoinduced electron transfer reactions in Eo^{2-}-α-Hb-Co(II) and Eo^{2-}-*β*-Hb-Co(II) were characterized by time-resolved laser flash photolysis, as described earlier for Eo^{2-}-Mb-Co(II). For quantitative characterization of the photoinduced electron transfer in the two photoenzymes, two reference proteins, lacking the Co(II)-protoporphyrin centers, Eo^{2-}-apo-α-Hb and Eo^{2-}-apo-*β*-Hb were prepared. These chromophore-modified proteins were prepared by reacting apo-α-Hb and apo-*β*-Hb with (**4**) under similar conditions used for the preparation of Eo^{2-}-α-Hb-Co(II) and Eo^{2-}-*β*-Hb-Co(II). Upon excitation of Eo^{2-}-apo-*β*-Hb, the bleached ground-state at $\lambda = 520$ nm and the formation of the $^{T}Eo^{2-}$-apo-*β*-Hb, at $\lambda = 580$ nm, were observed. No self-quenching photoproducts, $Eo^{\bullet -}$ and $Eo^{\bullet 3-}$ are detected. Similar transient species are observed for Eo^{2-}-apo-α-Hb. Thus, in the single chromophore-modified α-Hb and *β*-Hb the self-quenching electron transfer routes are eliminated.

Photoexcitation of Eo^{2-}-*β*-Hb-Co(II) results in a transient spectrum, that includes the bleached ground-state, $\lambda = 520$ nm, the $^{T}Eo^{2-}$ at $\lambda = 560$ nm and an additional species at $\lambda = 400$ nm (not observed in Eo^{2-}-apo-*β*-Hb) that corresponds to the reduced Co(I)-protoporphyrin IX center. Thus, photoexcitation of Eo^{2-}-*β*-Hb-Co(II) results in the transient formation of electron transfer products. Figure 11(A) shows the transient decay of $^{T}Eo^{2-}$-*β*-Hb-Co(II). The decay is single-exponential with a time constant $k_{T,obs} = 7.7 \times 10^3\ s^{-1}$. Formation of the Co(I) species implies that the oxidative electron transfer in $^{T}Eo^{2-}$-Mb-Co(II) occurs. We prefer, however, not to use the comparison of the

$$^{T}Eo^{2-}\text{-}\beta\text{-Hb-Co(II)} \xrightarrow{k_q = 1.8 \times 10^3\ s^{-1}} Eo^{\bullet -}\text{-}\beta\text{-Hb-Co(I)} \quad (20)$$

decay time-constants of $^{T}Eo^{2-}$-*β*-Hb-Co(II) and $^{T}Eo^{2-}$-apo-*β*-Hb for quantitative determination of the quenching rate constant. The chromophore microenvironment in apo-*β*-Hb could substantially differ from its surroundings in Eo^{2-}-*β*-Hb-Co(II) due to different structures of the proteins. Such different microenvironments could substantially influence the native decay of the excited chromophore. The quenching rate constant, eq 20, will be elucidated later by an alternative procedure. The formation of the Co(I) species, $\lambda = 400$ nm, indicates, however, that an oxidative electron transfer quenching mechanism is operative. Figure 11(B) shows the transient decay of the Co(I) species as a result of the back electron transfer, eq 21. The decay is single-exponential with a back electron transfer rate-constant corresponding to $k_b = 370\ s^{-1}$.

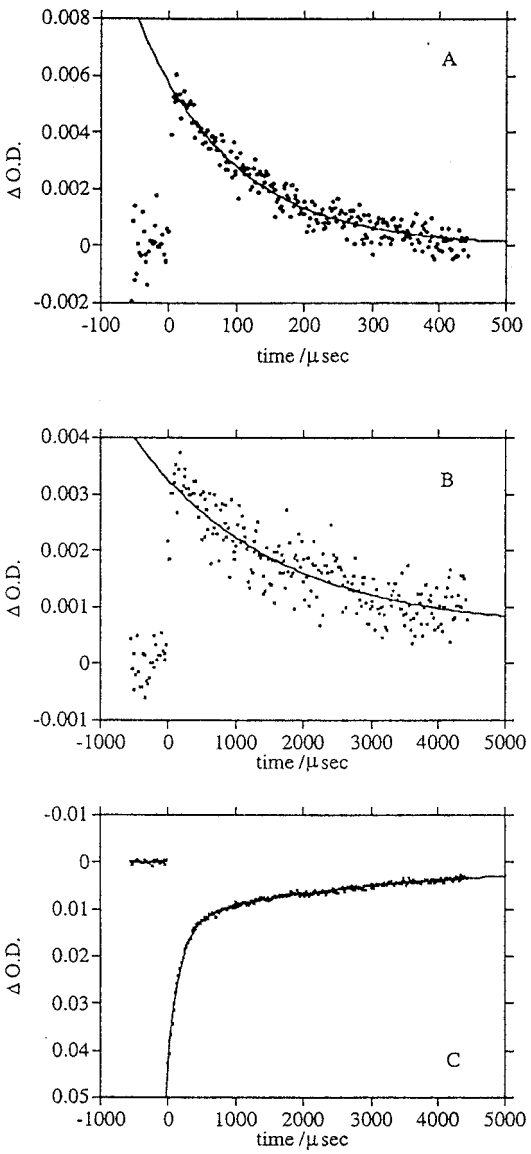

Figure 11. Transient absorbance changes upon photoexcitation of Eo^{2-}-*β*-Hb-Co(II), 0.17 mg·mL^{-1} in 0.1 M phosphate buffer, pH = 7.5: (A) Decay of the eosin triplet followed at $\lambda = 590$ nm. (B) Decay of Co(I) species followed at 400 nm. (C) Recovery of the eosin ground state followed at 510 nm.

$$Eo^{\bullet -}\text{-}\beta\text{-Hb-Co(I)} \xrightarrow{k_b = 370\ s^{-1}} Eo^{2-}\text{-}\beta\text{-Hb-Co(II)} \quad (21)$$

If the $^{T}Eo^{2-}$-*β*-Hb-Co(II) decays by two routes, i.e., native triplet decay and electron transfer quenching, then the recovery of the ground state Eo^{2-}-*β*-Hb-Co(II) should consist of the two transient populations ($^{T}Eo^{2-}$-*β*-Hb-Co(II) and $Eo^{\bullet -}$-*β*-Hb-Co(I)). Figure 11(C) shows the recovery of the bleached ground-state, $\lambda = 510$ nm, upon excitation of the system. The transient that restores the ground-state does not fit a single exponential process but fits a biexponential kinetics, implying the presence of two different populations that restore the ground-state. One population, $\phi_{fast} = 0.73 \pm 0.02$, restores the ground

(33) (a) Smyth, D. G.; Blumenfeld, O. O.; Konigsberg, W. *Biochem. J.* **1964**, *91*, 589. (b) Ishi, Y.; Lehrer, S. S. *Biophys. J.* **1986**, *50*, 75−80.

Table 1. Kinetic Parameters and Quantum Yields in the Electron Transfer of Eo^{2-}-α-Hb-Co(II) and Eo^{2-}-β-Hb-Co(II)

	Eo^{2-}-α-Hb-Co(II)	Eo^{2-}-β-Hb-Co(II)
k_q s^{-1}	6.5×10^3	1.8×10^3
ϕ_q	0.13	0.25
k_b s^{-1}	3.4×10^3	0.37×10^3
k_T s^{-1}	43×10^3	5.9×10^3
ϕ_T	0.87	0.75

state with a fast rate constant, $k_{fast} = 5900 \pm 50$ s^{-1}, whereas the second population, $\phi_{slow} = 0.27 \pm 0.02$, restores the ground-state with a slow rate constant, $k_{slow} = 370 \pm 20$ s^{-1}. The slow rate-constant that regenerates the ground-state coincides with the back electron transfer rate-constant, eq 21, determined by following the decay of Co(I), and hence the population (27%) regenerating the ground-state by the slow path is attributed to $Eo^{\bullet -}$-β-Hb-Co(I). The population (73%) restoring the ground-state by the fast route is thus attributed to the native decay of $^{T}Eo^{2-}$-β-Hb-Co(II). Thus, the native decay of $^{T}Eo^{2-}$-β-Hb-Co(II) is $k_T = 5900$ s^{-1}. The triplet decay of Eo^{2-}-β-Hb-Co(II), Figure 11(A), represents the observed decay rate-constant, $k_{T,obs}$ which represents the sum of native and quenching paths, $k_{T,obs} = k_T + k_q$. Since k_T and $k_{T,obs}$ were determined by analyzing the transients shown in Figure 11(C) and Figure 11(A), respectively, the derived quenching rate constant, eq 20, corresponds to $k_q = 1.8 \times 10^3$ s^{-1}. The electron-transfer quenching rate-constant is of similar magnitude as the native decay of the excited chromophore in $^{T}Eo^{2-}$-β-Hb-Co(II). Thus, the fraction of excited chromophore that will lead to electron transfer products is given by $\phi_q = k_q/(k_q + k_T)$, where the fraction of excited chromophore that decays naturally without electron transfer is given by $\phi_T = k_T/(k_q + k_T)$. Substitution of the respective rate constant yields $\phi_q = 0.25$ and $\phi_T = 0.75$. These fractions are identical to the ratio of the two populations that restore the bleached ground-state, as analyzed by the biexponential transient shown in Figure 11(C). These results support our conclusion that the ground-state is regenerated by the two complementary routes: the native decay of $^{T}Eo^{2-}$-β-Hb-Co(II) and back electron transfer of $Eo^{\bullet -}$-β-Hb-Co(I). Scheme 2 summarizes the sequence of electron-transfer processes that proceed upon excitation of Eo^{2-}-β-Hb-Co(II).

A similar set of experiments was performed with the Eo^{2-}-α-Hb-Co(II) and the respective reference compound Eo^{2-}-apo-α-Hb. The decay of $^{T}Eo^{2-}$-α-Hb-Co(II) is single-exponential with an observed rate constant of $k_{T,obs} = 4.95 \times 10^4$ s^{-1}. The derived values of the rate constants for the electron transfer quenching, native decay of the excited triplet and back electron transfer, are summarized in eqs 22−24. Table 1 summarizes the rate constants for oxidative electron transfer quenching of the two photoenzymes, Eo^{2-}-α-Hb-Co(II) and Eo^{2-}-β-Hb-Co(II) and the fractions of electron transfer products formed and their recombination rates in the two photoenzymes. The

$$^{T}Eo^{2-}\text{-}\alpha\text{-Hb-Co(II)} \xrightarrow{k_q = 6.5 \times 10^3\ s^{-1}} Eo^{\bullet -}\text{-}\alpha\text{-Hb-Co(I)} \quad (22)$$

$$^{T}Eo^{2-}\text{-}\alpha\text{-Hb-Co(II)} \xrightarrow{k_T = 4.3 \times 10^4\ s^{-1}} Eo^{2-}\text{-}\alpha\text{-Hb-Co(II)} \quad (23)$$

$$Eo^{\bullet -}\text{-}\alpha\text{-Hb-Co(I)} \xrightarrow{k_b = 3.4 \times 10^3\ s^{-1}} Eo^{2-}\text{-}\alpha\text{-Hb-Co(II)} \quad (24)$$

triplet excited state in $^{T}Eo^{2-}$-α-Hb-Co(II) decays 7-fold faster than in $^{T}Eo^{2-}$-β-Hb-Co(II). This can be attributed to different environments of the eosin chromophore in the two photoenzymes. The electron transfer quenching and back-electron transfer rates are slower in Eo^{2-}-β-Hb-Co(II) than in Eo^{2-}-α-Hb-Co(II). The $\Delta G°$ for the electron transfer reactions and the

Figure 12. Two-dimensional X-ray image of native β-Hb (from bovine). The Fe(II)-protoporphyrin IX and the cysteine 93 are marked in bold. The distance between the S-atom of the cysteine 93 residue and the metal center at the porphyrin site is calculated to be 12.87 Å.

reorganization energy, λ, accompanying electron transfer, are expected to be similar in the two photoenzymes. Hence, the differences in quenching rates and back electron transfer rates can be attributed to different donor−acceptor distances in the two photoenzymes (vide infra). Of specific importance is to note the long lifetime ($\tau = 2700$ μs) of the redox photoproducts $Eo^{\bullet -}$-β-Hb-Co(I).

Figure 12 shows the two-dimensional image of the X-ray structure of native β-Hb-Fe(II). Assuming that reconstitution of β-Hb with Co(II)-protoporphyrin IX does not alter the protein structure, and realizing that the chemical modification of the protein occurs site-specifically at cysteine residue 93, then the distance between the eosin chromophore and the Co(II)-protoporphyrin IX acceptor site is estimated to be $d = 12.87$ Å. The observed electron-transfer rates in Eo^{2-}-β-Hb-Co(II) and Eo^{2-}-α-Hb-Co(II) will be analyzed in terms of the Marcus theory[2b] in an attempt to elucidate the chromophore modification site in Eo^{2-}-α-Hb-Co(II).

Marcus relation of long-range electron transfer rates, k_{ET}, in donor−acceptor pairs is given by eq 25, where $\Delta G°$ is the free energy change accompanying electron transfer, λ is the reorganization energy, $H°_{AB}$ is the electronic coupling constant of the donor−acceptor pair at a van der Waals distance, ($d_o = 3$ Å), d is the distance separating the donor−acceptor pair, and β is the decay-constant of the electronic coupling as a function of distance. As the chromophore and electron acceptor sites in

$$k_{ET} = \left(\frac{4\pi^3}{h^2 \cdot \lambda \cdot k_B T}\right)^{1/2} \cdot H°_{AB} \cdot \exp\{-\beta(d - d_o)\} \cdot \exp\left\{-\frac{(\Delta G° + \lambda)^2}{4\lambda k_B T}\right\} \quad (25)$$

Eo^{2-}-α-Hb-Co(II) and Eo^{2-}-β-Hb-Co(II) are identical, the free energy changes accompanying the electron-transfer quenching, $\Delta G°_q$, and back electron transfer, $\Delta G°_b$, in the two photoenzymes are identical. The reduction potential of Co(II)-protoporphyrin IX in the reconstituted proteins is $E°_{Co(II)/Co(I)} = 0.61$ V, and the reduction potential of the $^{T}Eo^{2-}$ chromophore and the oxidized chromophore $Eo^{\bullet -}$ are $E° = -0.90$ V and $E°$

= 1.10 V, respectively.[35] Using these values, the free energy changes accompanying the electron transfer quenching, eq 26, and back electron transfer, eq 27, were calculated for the two

$$^{T}Eo^{2-}\text{-}\alpha/\beta\text{-Hb-Co(II)} \rightarrow Eo^{\bullet-}\text{-}\alpha/\beta\text{-Hb-Co(I)} \quad \Delta G^{\circ}_{q} = -0.6\ \text{eV} \quad (26)$$

$$Eo^{\bullet-}\text{-}\alpha/\beta\text{-Co(I)} \rightarrow Eo^{2-}\text{-}\alpha/\beta\text{-Hb-Co(II)} \quad \Delta G^{\circ}_{b} = -1.7\ \text{eV} \quad (27)$$

photoenzymes. In each of the two photoenzymes, Eo^{2-}-α-Hb-Co(II) or Eo^{2-}-β-Hb-Co(II), the electron transfer proceeds at fixed distances, (d), characteristic for each of the proteins. For each of the enzymes, two experimental electron transfer rate-constants are known (electron transfer quenching, k_q, and back electron transfer, k_b). Thus, the reorganization energy, λ, involved in the electron transfer in each of the photoenzymes can be calculated by eq 28.

$$\lambda = \frac{\Delta G_b^{\circ 2} - \Delta G_q^{\circ 2}}{4k_B T\left\{\ln\frac{k_q}{k_b} - \frac{\Delta G_b^{\circ} - \Delta G_q^{\circ}}{2k_B T}\right\}} \quad (28)$$

By substitution of the respective rate constants and free energy values, the reorganization energies for electron transfer in Eo^{2-}-α-Hb-Co(II) and Eo^{2-}-β-Hb-Co(II) were calculated to be λ_α = 1.15 ± 0.1 eV and λ_β = 1.1 ± 0.1 eV. The reorganization energies accompanying electron transfer in the two photoenzymes appear to be similar. This is reasonable as the donor−acceptor pair in the two photoenzymes are identical.

In the photoenzyme Eo^{2-}-β-Hb-Co(II) the distance between the chromophore site and the Co(II)-acceptor center is d_β = 12.87 Å. Since the reorganization energy is λ_β = 1.1 eV and the free energy-change for the electron transfer quenching is ΔG_q° = −0.6 eV, the decay constant of the electron coupling, β, can be calculated using eq 29. The derived value is β = 1.35 $Å^{-1}$. A similar value is obtained upon using k^{β}_{b} and the free-energy change ΔG° associated with the back electron transfer. The electronic coupling decay constant β depends on

$$k_q^{\beta} = 10^{13}\cdot\exp\{-\beta(d-3)\}\cdot\exp\left\{-\frac{(\Delta G^{\circ}+\lambda)^2}{4\lambda k_B T}\right\} \quad (29)$$

the nature of the donor−acceptor pair. Thus, a similar β value should accompany the electron transfer in Eo^{2-}-α-Hb-Co(II). The values ΔG°_{q} (or ΔG°_{b}), λ and β are identical in the two photoenzymes Eo^{2-}-β-Hb-Co(II) and Eo^{2-}-α-Hb-Co(II), and the only difference is the donor−acceptor distance at which electron transfer occurs. This allows us to estimate the donor−acceptor distance in the photoenzyme Eo^{2-}-α-Hb-Co(II) using the experimental ratio $k^{\beta}_{q}/k^{\alpha}_{q}$ (or $k^{\beta}_{b}/k^{\alpha}_{b}$) and eq 29 as outlined in eq 30 or eq 31. By substitution of the respective values, the electron-transfer distance (or donor−acceptor separation) d_α = 11.2 (±0.1) Å is obtained. The eosin chromophore in Eo^{2-}-α-Hb-Co(II) substitutes one of the lysine-sites. Figure 13 shows the two-dimensional X-ray structure of α-Hb and the 11 lysine residues present in the protein are marked. Lysine residue, Lys-90, is located at a distance of d = 11.10 Å that is

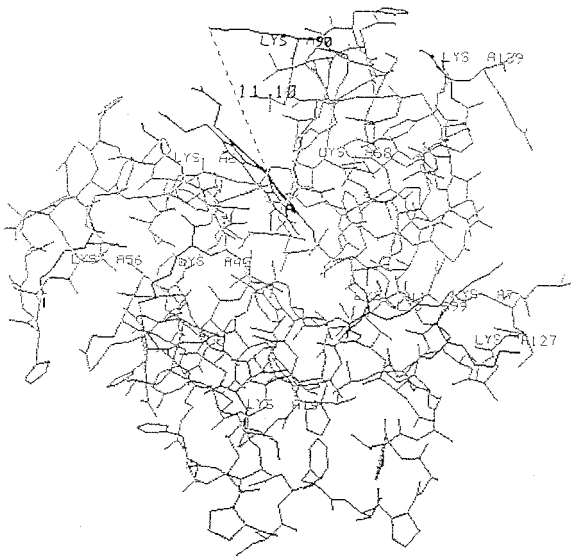

Figure 13. Two-dimensional X-ray image of native α-Hb (from bovine). The Fe(II)-protoporphyrin IX and the 11 lysine residues are marked in bold. The distance between the ϵ-nitrogen atom of lysine 90 to the metal center of the porphyrin is 11.10 Å.

$$\frac{k_q^{\beta}}{k_q^{\alpha}} = \exp\{-(d_\beta - d_\alpha)\} \quad (30)$$

$$d_\alpha = d_\beta + \frac{1}{\beta}\cdot\ln\frac{k_q^{\beta}}{k_q^{\alpha}} \quad (31)$$

closest to the calculated electron-transfer distance. Thus, the kinetic analysis suggests that the chromophore is associated with the Lys-90 position in Eo^{2-}-α-Hb-Co(II). The structure of α-Hb, Figure 13, indicates that Lys-90 is located at the exterior periphery of the protein and that the amino residue is not sterically hindered by the protein matrix. We suggest that the structurally nonhindered position of Lys-90 at the protein periphery leads to kinetic preference of modification by **4**, and hence to a single chromophore-modified photoenzyme, Eo^{2-}-α-Hb-Co(II).

The detailed analyses of the photoinduced electron transfer in Eo^{2-}α-Hb-Co(II) and $Eo^{2-}$$\beta$-Hb-Co(II) revealed that in the two reconstituted proteins oxidative quenching yields the intermediate electron transfer products $Eo^{\bullet-}$-α/β-Hb-Co(I). This suggests that the two reconstituted proteins could act as hydrogenation biocatalysts in the presence of the sacrificial electron donor, Na_2EDTA, eq 32 and eq 33. Figure 14 shows the rate of ethylene formation upon steady-state irradiation of Eo^{2-}-α-Hb-Co(II) and Eo^{2-}-β-Hb-Co(II) in the presence of Na_2-EDTA under a saturated atmosphere of acetylene. The quantum yield for ethylene formation corresponds to ϕ = 0.02 for Eo^{2-}-

$$Eo^{\bullet-}\text{-}\alpha/\beta\text{-Hb-Co(I)} + Na_2EDTA \rightarrow Eo^{2-}\text{-}\alpha/\beta\text{-Hb-Co(I)} + NaEDTA_{ox} \downarrow \text{oxidation products} \quad (32)$$

$$Eo^{2-}\text{-}\alpha/\beta\text{-Hb-Co(I)} + H^{+} \rightarrow Eo^{2-}\text{-}\alpha/\beta\text{-Hb-Co(III)-H} \quad (33)$$

$$Eo^{2-}\text{-}\alpha/\beta\text{-Hb-Co(III)-H} + C_2H_2 \xrightarrow{H^+} Eo^{2-}\text{-}\alpha/\beta\text{-Hb-Co(III)} + C_2H_4 \quad (34)$$

α-Hb-Co(II) and ϕ = 0.004 Eo^{2-}-β-Hb-Co(II). Control experi-

(34) The specific modification of cysteine-93 residue of β-Hb-Co(II) by eosin was further supported by titration of β-Hb-Co(II) and Eo^{2-}-β-Hb-Co(II) with 5,5′-dithiobis(2-nitrobenzoic) acid (Ellman's reagent). While β-Hb-Co(II) contains a single free cysteine residue, no free cysteine was detected for Eo^{2-}-β-Hb-Co(II).

(35) (a) Moser, J.; Grätzel, M. *J. Am. Chem. Soc.* **1984**, *106*, 6557−6564. (b) Kepka, A. G.; Grossweiner, L. I. *Photochem. Photobiol.* **1971**, *14*, 621−639.

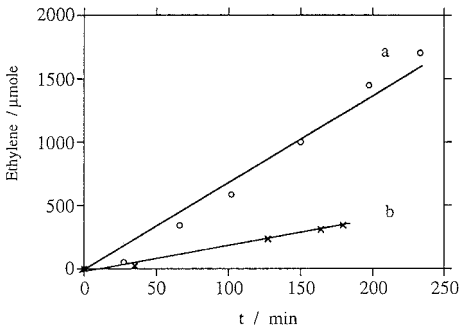

Figure 14. Rate of acetylene hydrogenation to ethylene at time intervals of illumination ($\lambda > 475$ nm) of (a) Eo^{2-}-α-Hb-Co(II), 0.17 mg·mL^{-1} and (b) Eo^{2-}-β-Hb-Co(II), 0.17 mg·mL^{-1}. All systems include Na_2-EDTA, 0.01 M, and are saturated with acetylene. Experiments were performed in 3 mL 0.1 M phosphate buffer, pH = 7.5.

Scheme 2. Electron Transfer Pathways upon Photoexcitation of Eo^{2-}-β-Hb-Co(II)

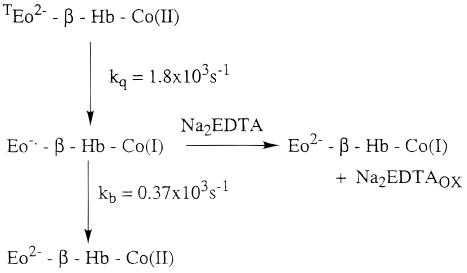

ments revealed that no photohydrogenation of acetylene takes place in the absence of Na_2EDTA, or upon application of the reconstituted Co(II)-proteins lacking the Eo^{2-}-chromophore, α/β-Hb-Co(II), or upon application of the respective eosin-modified apo-proteins lacking the Co(II)-protoporphyrin sites, Eo^{2-}-apo-α/β-Hb. These experiments confirm that electron transfer from the excited eosin chromophore to the Co(II)-protoporphyrin IX sites, and subsequent scavenging of the oxidized photoproduct by Na_2EDTA, are essential processes to induce the photohydrogenation of acetylene to ethylene.

Cyclic Photosynthetic Systems through Application of the Eo^{2-}-Mb-Co(II) Photoenzyme. The detailed analysis of the photoinduced electron transfer in Eo^{2-}-Mb-Co(II) and Eo^{2-}-α/β-Hb-Co(II) revealed the important conclusion that the primary redox photoproducts exhibit a relatively long lifetime. The lifetime of $Eo^{\bullet-}$-Mb-Co(I) was found to be 7 μs and of $Eo^{\bullet-}$-α-Hb-Co(I) and $Eo^{\bullet-}$-β-Hb-Co(I) 300 μs and 2700 μs, respectively. The stability of the electron transfer products is attributed to the rigid protein structures that spatially separate the oxidized photoproduct from the reduced species. The oxidized chromophore is anticipated to be located at the protein periphery, whereas the Co(I)-protoporphyrin IX site is embedded in the protein. In this configuration, it is expected that a diffusional *reversible* electron donor could be oxidized by the oxidized chromophore. Diffusional electron mediators usually do not electrically communicate with redox centers embedded in proteins, unless specific channels allow the penetration of the redox mediator into the protein. Thus, oxidation of the diffusional electron mediator by the oxidized chromophore could further separate the redox species and assist in their stabilization against back-electron transfer, Figure 15. Introduction of a second oxidative protein (enzyme) that recognizes the oxidized diffusional electron mediator could then stimulate the oxidation of the substrate which is specific to the second protein. Thus, by coupling a reductive photoenzyme and an oxidative biocatalyst through a diffusional electron mediator, cyclic photosynthetic transformations could be induced.

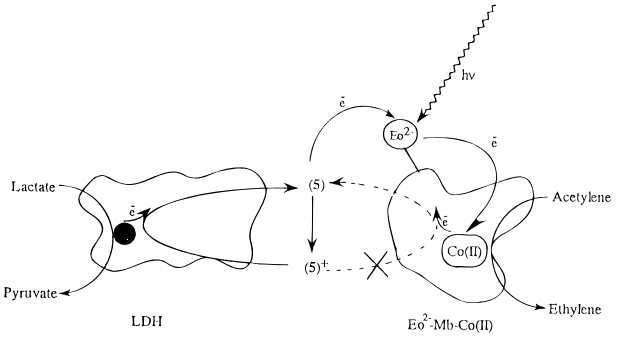

Figure 15. Scheme of electron transfer pathway for cyclic photoinduced hydrogenation of acetylene by lactate using Eo^{2-}-Mb-Co(II) and LDH as biocatalyst.

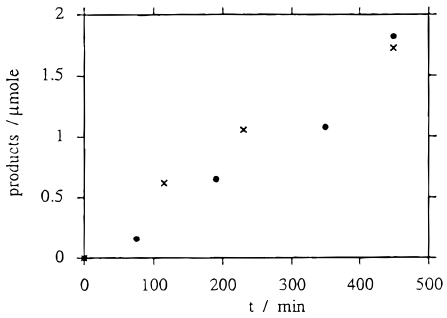

Figure 16. Rates of formation of products upon illumination of a photosystem, 3 mL, phosphate buffer, 0.1 M, pH = 7.4, that includes Eo^{2-}-Mb-Co(II), 0.11 mg·mL^{-1}, LDH, 0.6 units·mL^{-1}, **5**, 8×10^{-3} M and lactic acid, 10^{-2} M, under atmospheric pressure of acetylene: (●) rate of ethylene formation (×) rate of pyruvic acid formation.

As a model system that operates according to this principle, the photoenzyme Eo^{2-}-Mb-Co(II) as a reductive site was coupled to lactate dehydrogenase, LDH, using *N*-methylferrocene caproic acid (**5**) as diffusional electron carrier, Figure 15. Lactate dehydrogenase, LDH (E.C. 1.1.2.3) is a flavocytochrome b_2 enzyme composed of four subunits, 230 Kd. Each of the tetramer units includes an Fe(II)-prophyrin and FAD site.[36] The enzyme biocatalyzes the oxidation of lactic acid and cytochrome *c* acts as a native electron carrier for LDH.[37] Steady-state irradiation, $\lambda > 475$ nm, of a photosystem that includes Eo^{2-}-Mb-Co(II), LDH, *N*-methylferrocene caproic acid (**5**), and the substrates acetylene and lactic acid for the respective two biocatalysts, results in the formation of ethylene (reduction product) and pyruvic acid (oxidation product). Figure 16 shows the rate of ethylene evolution and pyruvic acid formation at time intervals of illumination. The rates of formation of the two products is identical and they are formed in an equimolar ratio. Since the hydrogenation of acetylene, eq 35, and oxidation of lactic acid, eq 36, represent two-electron redox reactions,

$$H-C\equiv C-H + 2e^- + 2H^+ \longrightarrow C_2H_4 \qquad (35)$$

$$CH_3-\underset{\displaystyle OH}{\underset{|}{CH}}-CO_2H \longrightarrow CH_3-\overset{\displaystyle O}{\overset{\|}{C}}-CO_2H + 2e^- + 2H^+ \qquad (36)$$

the cyclic operation of the photosynthetic system, Figure 15, is expected to yield the products at a 1:1 molar ratio. The quantum yields for the formation of the products corresponds to $\phi = 2 \times 10^{-3}$. From the number of moles of products formed in the photosystem after 450 min of irradiation, the total turnover numbers (TTN) of LDH and Eo^{2-}-Mb-Co(II) were calculated to be 70 and 120, respectively. This indicates that the biocatalysts are recycled in the light-induced chemical transformations. Control experiments revealed that all of the

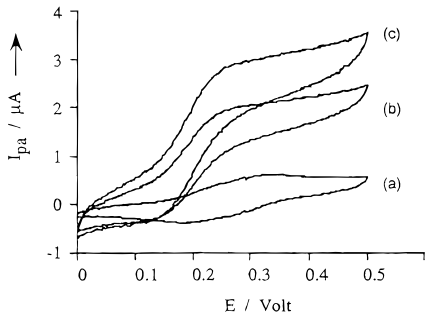

Figure 17. Cyclic voltammograms of an electrolyte solution composed of 0.01 M phosphate buffer and Na_2SO_4, 0.1 M, that includes LDH 0.15 units·mL^{-1} and *N*-methylferrocene caproic acid (**5**) 3×10^{-4} M (a) without added lactate; (b) in the presence of lactate, 2×10^{-3} M; and (c) with lactate 1×10^{-2} M. All experiments were recorded under Ar, scan rate 2 mV·s^{-1}. A Au-electrode was used as working electrode and SCE as reference electrode.

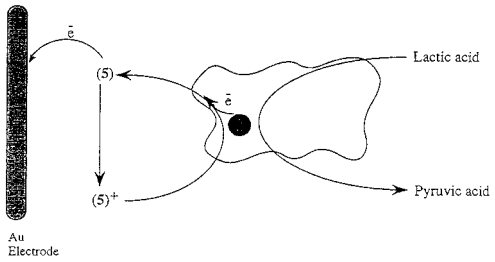

Figure 18. Electrobiocatalayzed oxidation of lactate by LDH in the presence of the diffusional electron mediator (**5**).

components were essential to stimulate the evolution of C_2H_4 and formation of pyruvic acid. Exclusion of the electron mediator (**5**) or LDH prevented the formation of pyruvic acid. These control experiments suggest that the electron carrier (**5**) is essential to couple the reductive photoenzyme Eo^{2-}-Mb-Co(II) and LDH and implies that LDH acts as the biocatalyst for the oxidation of lactic acid.

The detailed electron transfer features of the cyclic photosynthetic system were characterized by time-resolved laser photolysis and electrochemical means. The photoinduced intraprotein electron transfer reactions in Eo^{2-}-Mb-Co(II) were characterized earlier (vide supra). To account for the electron-transfer processes in the cyclic photosystem, Figure 15, the secondary electron transfer between the primary photoproducts $Eo^{\bullet -}$-Mb-Co(I) and the electron carrier (**5**) needs characterization. Also, the oxidation of lactic acid by LDH in the presence of the oxidized electron mediator (**5**) requires experimental and mechanistic support.

Figure 17 shows the cyclic voltammograms of *N*-methylferrocene caproic acid (**5**) in the presence of LDH, in the absence of lactic acid (curve a) and upon addition of lactic acid (curves b and c). Addition of lactic acid results in an electrocatalytic anodic current at the characteristic oxidation potential of (**5**). The electrocatalytic anodic current increases as the concentration of lactic acid is elevated. Control experiments revealed that no electrocatalytic anodic currents are observed when the redox-mediator or LDH are excluded from the electrolyte. These experiments clearly indicate that the oxidized electron carrier is recognized by LDH and that it mediates the biocatalyzed oxidation of lactic acid by LDH, Figure 18.

Our previous discussion emphasizes that upon excitation of Eo^{2-}-Mb-Co(II) the photoproducts $Eo^{\bullet -}$-Mb-Co(I) are formed and they recombine with a back electron transfer rate constant corresponding to 1.4×10^5 s^{-1}. Excitation of the Eo^{2-}-Mb-Co(I) in the presence of *N*-methylferrocene caproic acid (**5**) results in the transient absorption spectrum of the characteristic

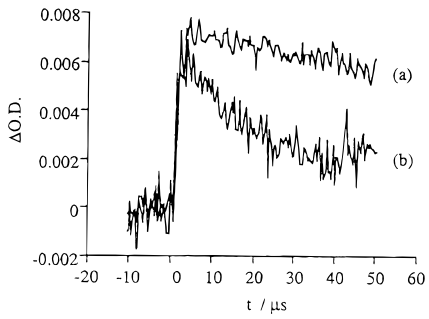

Figure 19. Transient decay of the photogenerated ferrocenylium cation, $\mathbf{5}^+$, (followed at $\lambda = 630$ nm): (a) in the presence of Eo^{2-}-Mb-Co(I), (b) after addition of LDH and lactate, 1×10^{-2} M.

absorption band of the ferrocenyl cation at $\lambda = 630$ nm. This result clearly indicates that the primary $Eo^{\bullet -}$-Mb-Co(I) was reduced by (**5**) to yield the ferrocenyl cation, eq 37. Figure 19 (curve a) shows the transient decay of the ferrocenyl cation, $(\mathbf{5})^+$, photoproduct as a result of back electron transfer to the Co(I) site, eq 38. The decay corresponds to a second-order process, $k_{bf} = 6.25 \times 10^5$ M^{-1}·s^{-1}. Photoexcitation of a system that includes Eo^{2-}-Mb-Co(II), **5**, and LDH yields the ferrocenyl cation that decays much faster, Figure 19 (curve b). The observed second-order decay rate-constant for the ferrocenyl cation in the presence of LDH is $k_{obs} = 1.6 \times 10^7$ M^{-1}·s^{-1}. The enhanced decay rate of the ferrocenyl cation in the presence of LDH is consistent with the mediated oxidation of LDH by the ferrocenyl cation, eq 39. Thus, the recombination of the oxidized ferrocenyl cation and the oxidation of LDH by $(\mathbf{5})^+$ provide two routes for depletion of the oxidized electron carrier ($k_{obs} = k_{bf} + k_{ox}$). By substitution of the back electron transfer rate-constant of $(\mathbf{5})^+$ with the Co(I) species, eq 38, the bimolecular rate constant for the oxidation of LDH by the ferrocenyl cation, eq 39, is estimated to be $k_{ox} = 1.5 \times 10^7$ M^{-1}·s^{-1}. This kinetic analysis clearly demonstrates that the oxidation of LDH by the photogenerated ferrocenyl cations is kinetically favored (ca. 10^2-fold as compared to the recombination rate of $(\mathbf{5})^+$ with the reduced Co(I) site).

$$Eo^{\bullet -}\text{-Mb-Co(I)} + Fc \rightarrow Eo^{2-}\text{-Mb-Co(I)} + Fc^+ \quad (37)$$

$$Eo^{2-}\text{-Mb-Co(I)} + Fc^+ \xrightarrow{k_{bf} = 6.25 \times 10^5\ M^{-1}\cdot s^{-1}} Eo^{2-}\text{-Mb-Co(II)} + Fc \quad (38)$$

$$LDH + Fc^+ \xrightarrow{k_{ox} = 1.5 \times 10^7\ M^{-1}\cdot s^{-1}} LDH_{ox} + Fc \quad (39)$$

Figure 20 shows the transient recovery of the bleached ground-state eosin ($\lambda = 510$ nm) upon photoexcitation of Eo^{2-}-Mb-Co(II) in the presence of *N*-methylferrocene caproic acid (**5**). This recovery of the ground-state chromophore should be compared to the transient shown in Figure 5(B), where the recovery of the bleached eosin is followed as a result of the photoexcitation of Eo^{2-}-Mb-Co(II) alone. The bleached ground-state chromophore in the presence of the ferrocene electron carrier is recovered by a very rapid process, much faster than the characteristic recovery of Eo^{2-}-Mb-Co(II) due to the

(36) (a) Jacq, C.; Lederer, F. *Eur. J. Biochem.* **1974**, *41*, 311−320. (b) Labeyrie, F.; Baudras, A.; Lederer, F. In *Methods in Enzymology*; Fleischer, S., Packer, L., Eds.; Academic Press: New York, 1978; Vol. 53; pp 238−256.

(37) (a) Amine, A.; Deni, J.; Kauffmann, J.-M. *Bioelectrochem. Bioenerg.* **1994**, *34*, 123−128. (b) Cass, A. E. G.; Davis, G.; Hill, H. A. O.; Nancarrow, D. J. *Biochim. Biophys. Acta* **1985**, *828*, 51−57. (c) Cass, A. E. G.; Davis, G.; Green, M. J.; Hill, H. A. O. *J. Electroanal. Chem.* **1985**, *90*, 117−127.

(38) Pfennig, N. In *The Photosynthetic Bacteria*; Clayton, R. K., Sistrom, W. R., Eds.; Plenum Press: New York, 1978; Chapter 1, p 8.

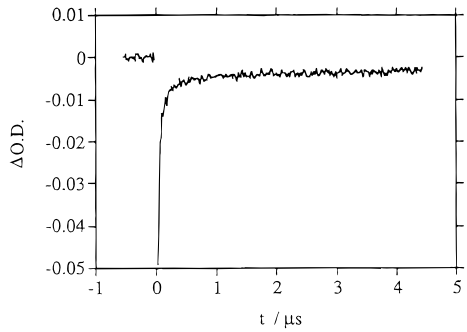

Figure 20. Transient recovery of eosin ground-state of Eo^{2-}-Mb-Co(II), followed at $\lambda = 510$ nm, in the presence of **5**, 8×10^{-3} M.

intramolecular recombination. The recovery of the ground-state eosin chromophore in the presence of **5** proceeds by two complementary routes, eq 40. One route involves the intramolecular back electron transfer and the second path involves the oxidation of the diffusional ferrocene component by the oxidized chromophore. The lifetime of the oxidized chromophore in the presence of the ferrocene electron mediator is 0.06 μs that corresponds to an observed rate-constant for the recovery of the eosin chromophore of $k_{obs} = 1.7 \times 10^7$ s^{-1}. Since the intramolecular back electron transfer rate constant is $k_b = 1.4 \times 10^5$ s^{-1}, the rate constant for the oxidation of the electron mediator by the oxidized eosin, k_{red}, is calculated to be $k_{red} = 2 \times 10^9$ $M^{-1}\cdot s^{-1}$ ($k_{obs} = k_b + k_{red}$[Fc]; [Fc] = 8×10^{-3} M).

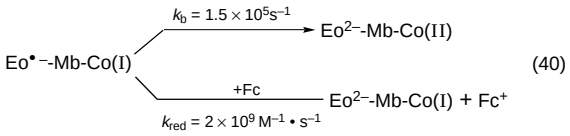

(40)

From the back electron transfer rate constant and the rate constant for the oxidation of the electron carrier, the fractions of the initial oxidized chromophore which are depleted by the recombination and oxidation of the ferrocene component, ϕ_{red}, are calculated to be $\phi_{red} = k_{red}$[Fc]$/k_{obs} = 0.94$ and $\phi_b = k_b/k_{obs} = 0.06$. We realize that the primary photoproducts are sufficiently stabilized to favor the oxidation of the diffusional electron mediator over the back electron transfer, and 94% of the primary oxidized photoproduct is depleted by the oxidation of the ferrocene component. This analysis allows us to summarize the electron transfer reactions in the cyclic photosystem that includes the two biocatalysts, Eo^{2-}-Mb-Co(II) and LDH, as outlined in Figure 15.

A vectorial electron transfer (or hole-transfer) between the reductive semisynthetic photoenzyme, Eo^{2-}-Mb-Co(II) and LDH proceeds in the photosystem and is mediated by the diffusional electron carrier N-methylferrocene caproic acid. The success in inducing this vectorial electron transfer originates from the stabilization of the primary redox products, $Eo^{\bullet -}$-Mb-Co(I), by the protein matrix and spatial separation of the redox intermediates. The rigid protein assembly provides the basic mechanism to retard the back electron transfer. This facilitates the secondary oxidation of (**5**) by the oxidized chromophore. The secondary electron transfer path adds further stability to the resulting redox species due to insulation of the Co(I)-species from the oxidized ferrocenylium cation product. This enables the oxidation of the redox-active center of LDH by $(\mathbf{5})^+$. The latter process yields long-lived, stable redox sites trapped in the two proteins. As a result of this, effective hydrogenation of acetylene at the Co(I) electron-trap and oxidation of lactic acid at the hole-trap occur.

Conclusions

We have presented a novel approach to tailor photoactive biocatalytic materials by reconstitution of native heme-proteins with Co(II)-protoporphyrin IX and chemical modification of the reconstituted proteins with a chromophore unit. Myoglobin, Mb, and α or β subunits of hemoglobin, Hb, were reconstituted with Co(II)-protoporphyrin IX and further modified with the eosin chromophore to yield a series of photocatalytic proteins, "photoenzymes", Eo^{2-}-Mb-Co(II), Eo^{2-}-α/β-Hb-Co(II). The series of chromophore-modified Co(II)-protoporphyrin IX reconstituted proteins reveal photocatalytic properties and induce under steady-state illumination the photohydrogenation of acetylene to ethylene. Detailed kinetic analysis of the photohydrogenation of acetylenedicarboxylic acid by Eo^{2-}-Mb-Co(II) reveals that the semisynthetic protein follows the Michaelis−Menten kinetic model.

The light-induced electron transfer paths in the series of photoenzymes was characterized by time-resolved laser photolysis experiments. In all of the proteins, oxidative electron-transfer quenching of the excited triplet eosin by the Co(II)-protoporphyrin IX site was observed, and the formation of the redox species $Eo^{\bullet -}$-Mb-Co(I) and $Eo^{\bullet -}$-α/β-Hb-Co(I) was established. The electron transfer reactions in the site-specific modified photoenzymes Eo^{2-}-α-Hb-Co(II) and Eo^{2-}-β-Hb-Co(II) were analyzed in terms of Marcus theory. This allowed us to elucidate the structural features of the photoenzyme Eo^{2-}-α-Hb-Co(II).

The redox species formed upon photoinduced electron transfer in the series of photoenzymes revealed high stability against back electron transfer. This was attributed to the spatial separation of the redox intermediates by the rigid protein assembly. The pronounced stability of the primary redox intermediates allowed us to couple the reductive photoenzyme Eo^{2-}-Mb-Co(II) with an oxidative enzyme lactate dehydrogenase, LDH, using a diffusional redox carrier, *N*-methylferrocene caproic acid (**5**). The cyclic photohydrogenation of acetylene by lactate was accomplished in the photosystem that included the two biocatalysts. Interestingly, the photosynthetic bacteria chloroflexus uses lactate as the oxidation substrate, similar to the artificial system.[38] The detailed analysis of the vectorial electron transfer in the cyclic photosystem revealed enhancement in the stability of the oxidized and reduced intermediates formed. This was attributed to the higher degree of spatial separation of the redox species as a result of the sequential electron transfer reactions. This effect resembles the charge separation in the photosynthetic reaction center where vectorial electron transfer assists the stabilization of the redox intermediates. The method to tailor photoenzymes via reconstitution of native proteins and the coupling of two redox biocatalysts to stimulate cyclic photosynthesis open the possibility to organize a variety of new photosynthetic systems.

Acknowledgment. This research was supported in part by the Volkswagen Stiftung (Germany), by the James Frank Minerva Center and by the Research Institute of Innovative Technology for the Earth (RITE-NEDO), Japan.

Supporting Information Available: Absorption spectra of Mb-Co(II) and Eo^{2-}-Mb-Co(II); rate of hydrogen evolution by Eo^{2-}-Mb-Co(II); absorption spectra of α-Hb-Co(II) and β-Hb-Co(II); and transient absorption spectra of Eo^{2-}-α-Hb-Co(II) and Eo^{2-}-Apo-β-Hb (4 pages). See any current masthead page for ordering and internet access instructions.

JA9608712